Programmable promoter editing for precise control of transgene expression

Sneha R. Kabaria[1], Yunbeen Bae[1], Mary E. Ehmann[1], Adam M. Beitz[1], Brittany A. Dorn[1], Emma L. Peterman[1], Kasey S. Love[2], Deon S. Ploessl [1], Kate E. Galloway[1*]

1. Department of Chemical Engineering, MIT, Cambridge, MA 02139, USA
2. Department of Biological Engineering, MIT, Cambridge, MA 02139, USA
*Correspondence to: katiegal@mit.edu

Abstract

Subtle changes in gene expression direct cells to distinct cellular states. Identifying and controlling dose-dependent transgenes requires tools for precisely titrating expression. To this end, we developed a framework called DIAL for building editable promoters that allows for fine-scale, heritable changes in transgene expression. Using DIAL, we increase expression by recombinase-mediated excision of spacers between the binding sites of a synthetic zinc-finger transcription factor and the core promoter. By nesting varying numbers and lengths of spacers, DIAL generates a tunable range of unimodal setpoints from a single promoter construct. Through small-molecule control of transcription factors and recombinases, DIAL supports temporally defined, user-guided control of transgene expression. Integration of DIAL promoters into lentivirus allows for efficient delivery to primary cells. As promoter editing generates stable states, DIAL setpoints are heritable, facilitating mapping of transgene levels to phenotypes. The highly modular and extensible DIAL framework opens up new opportunities for screening and tailoring transgene expression to regulate gene and cell-based therapies.

Highlights

Promoter editing generates a range of unimodal setpoints from DIAL, a synthetic promoter system

Length of the excisable spacer and identity of the zinc-finger activator tune setpoints

Nested, excisable spacers expand the number of unimodal setpoints

DIAL generates stable setpoints that are robust to varying transactivator levels

DIAL transmits transient inputs into heritable states

The TET-DIAL system enables small molecule activation of defined setpoints

DIAL controls expression in primary cells and iPSCs; regulates physiologically-relevant transgenes

One Sentence Summary

DIAL offers an extensible framework for designing synthetic promoters that generate heritable setpoints of gene expression and performs across a range of cell types and delivery systems.

Main

Subtle changes in gene expression can generate diverging cell fates.[1–6] Overexpression of endogenous and synthetic genes drives and redirects native processes and can augment native cellular functions.[7–10] However, identifying which transgenes have these subtle effects requires fine-tuned control, and implementing control over dosage-sensitive regimes remains a challenge.[1,11] In particular, non-linear effects of gene expression can confound inference of positive and negative regulation of phenotypes.[1,2,12,13] Tools that support fine-scale titration of expression reveal non-monotonic relationships between expression of regulators and phenotypes.[1,2,12] While useful for identifying linear regulators, large-scale screening tools such as CRISPR-based knockout, knockdown, and activation often do not provide sufficient resolution to find regulators with non-linear relationships to phenotypes. Such CRISPR-based screening does not predict how overexpression of transgenes influences cellular behaviors.[14] As transgenes are increasingly used to augment cellular functions and program cell fate, there is a critical need for scalable tools to identify regulators with complex functions and define their influence on physiologically-relevant phenotypes.[14–17]

Tools that support titration may also enable tuning and control of transgene expression in therapeutic contexts for precision cell and gene therapy.[10] To this end , synthetic biology aims to harness the power of native biology by interfacing native and synthetic gene regulatory networks. Dynamic synthetic circuits such as toggle switches, pulse generators, bandpass filters, and oscillator can dynamically control transgene to direct prescribing cellular processes, states, and identities.[18–25] However, rational *de novo* design of synthetic circuits remains challenging. Even simple inducible promoters can exhibit emergent, undesirable behaviors that impede the development of transgenic systems and gene circuits.

Synthetic transcription factor systems offer constitutive and inducible control of gene expression.[10,12,26,27] Synthetic transcription factors mimic the DNA-binding and transcriptional activation of native TFs by modularly fusing high-affinity DNA-binding domains to strong transactivation domains. These synthetic TFs are often directed to binding sites upstream of a weak core promoter.[26–28] Properties of transcription factor binding sites, including number, spacing to the core promoter, and affinity for TFs, influence the recruitment of transcriptional machinery and thus the levels of transgene expression.[27] Within a limited range, increasing levels of synthetic transcription factors or small-molecule inducers can increase the mean level of expression across a population of cells.[29] However, these tools generally suffer from bimodal distributions of expression.[27,30] Bimodality limits robust control of the entire population and may confound construction of a functional relationship between expression and phenotypes. More complex circuits can linearize inducible systems to generate unimodal dose-responses at the cost of larger which may be difficult to translate to relevant cell type.[31]

To develop a flexible tool, we outlined a set of desirable features for a promoter system that would allow us to control transgenes over dosage-sensitive regimes to study and induce specific phenotypes. First, we want a system capable of generating tunable setpoints of transgene expression

that span physiologically-relevant ranges for titration from a single construct. Second, setpoints should be unimodal to ensure uniform induction and reliable control across an entire population of cells. Third, setpoints should be robust to fluctuations in levels of components such as synthetic transcription factors to ensure stable, homogenous output levels. Fourth, to map setpoint levels to phenotypes, setpoints should be recordable and heritable. As cell fates emerge over longer timescales, an ideal synthetic promoter system generates setpoints in gene expression via heritable changes that can be read at terminal timepoints. Fifth, for temporal control of induction, the system should be amenable to user-guided cues that implement reversible and irreversible changes in expression from a single construct. Finally, for translational impact, the synthetic promoter system should be compact for delivery into primary cells.

Here we expand the precision and tunability of synthetic promoters by developing a system capable of generating multiple setpoints of transgene expression from a single promoter. This promoter editing system called “DIAL” programs unimodal setpoints of transgene expression through a defined combination of inputs (Fig 1). Because the distance between synthetic transcription factor binding sites and core promoter impacts expression level, DIAL uses recombinase-based editing of the promoter to excise a spacer and increase expression. Editing generates distinct output setpoints pre- and post-excision. The length of the spacer tunes the output setpoint range of expression by reducing the expression of the pre-edited promoter. By layering orthogonal recombinase sites, we generate four stable setpoints from a single founder sequence. We demonstrate that DIAL setpoints are robust over a large range of transactivator levels. Additionally, DIAL translates user-defined inputs, including modRNA and small-molecules, into heritable setpoints. To further explore the generality of the spacer-excision architecture and to support stability and reversibility, we expanded DIAL to respond to the tetracycline-responsive transactivator, rtTA. TET-DIAL generates tetracycline-inducible, unimodal setpoints and allows independent tuning of the induced fraction of cells and mean levels of expression. Importantly, for broad translation to diverse cell types, we demonstrate that DIAL can be delivered via lentivirus and controls gene expression in induced pluripotent stem cells and primary cells.

Results

Promoter editing generates a range of unimodal setpoints

Native transcription factors commonly use zinc-finger (ZF) binding motifs to identify cognate binding sites across the genome. Synthetic ZF transcription factors (ZFas) are designed to bind arrays of unique binding sites orthogonal to native sequences. ZFas induce transcription by binding near core promoters via their ZF DNA binding domain and recruiting transcriptional machinery via their

transactivation domain (TAD). To compose the DIAL promoter system, we turned to a set of well-defined ZFas from the COMET tool kit.[26,27] We designed the DIAL promoter with an array of tessellated binding sites specific to two ZF domains (ZF43, ZF37) separated from a downstream of a minimal TATA promoter by a spacer (Fig 1B, Fig S1). Between the minimal promoter and binding site array, we placed a spacer flanked by loxP ("floxed") recognition sites. Recognition of loxP sites by Cre tyrosine recombinase edits the promoter by excising the floxed spacer. Spacer excision brings the binding site array closer to the minimal promoter. In the presence of the ZFa, excision increases expression from a low to a high setpoint (Fig 1B). In the absence of ZFa, expression is off. Using a combination of Cre and ZFa, we program three setpoints of gene expression from a single promoter sequence.

To characterize the DIAL framework, we transfected HEK293T cells with a DIAL promoter containing a spacer length of 203 bp. Through the combination of ZFa and recombinase editor inputs, we changed the molecular state of the reporter and induced unimodal off, low, and high setpoints of expression (Fig 1C, D, Fig S1-2). By co-expressing each ZFa with a fluorescent protein, we verified that the levels of ZFa do not change in response to Cre, showing that expression differences are not due to perturbations in levels of ZFa (Fig S3).

Cre-mediated excision of the spacer will increase expression by reducing the distance between the binding sites and minimal promoter. As expected, in the presence of ZFa, addition of Cre increases expression, reaching the level of a control promoter which lacks a spacer (Fig S3). We validated spacer excision via genotyping PCR. As expected, in the presence of Cre, a shorter band appears, corresponding to the edited promoter (Fig S4).

Next, we explored tuning the setpoints and range of the DIAL reporter. In synthetic promoter systems, expression decreases as the distance between the transcription factor binding sites and the transcription start site increases.[27] We hypothesized that increasing the length of the excisable spacer would further decrease the pre-excision setpoint, potentially increasing the overall fold-change accessible to DIAL. For a panel of spacers ranging from 27 bp to 263 bp, increasing spacer length decreases pre-excision output expression and increases output dynamic range (Fig 1E, Fig S5). Post-excision expression converges to the control construct consisting of the expected post-excision sequence (Fig 1E, Fig S5).

Our promoter responds to both ZF37 and ZF43, allowing us to modularly combine TADs of different strength with these targeting sequences. We found that TADs modestly tuned the DIAL setpoints with stronger ZF-TADs increasing the fold change in response to Cre (Fig 1F, Fig S5). The strongest ZFa, ZF37-VPR, substantially increased the range of expression but generated bimodal expression of the reporter, potentially limiting its utility for experiments requiring precise titration (Fig 1F).

To expand the number of setpoints possible with a single ZFa, we constructed a DIAL promoter with a nested set of excisible spacers. In this configuration, the original Cre-floxed spacer is modified to include internal, orthogonal VloxP sites, which can be independently recognized by a second tyrosine recombinase, VCre. Upon addition of VCre, a portion of the spacer is excised, and expression increases

from a low setpoint to a medium one. Upon addition of Cre, the entire spacer is excised and expression increases to a high setpoint (Fig 1H, Fig S6). Through addition of specific recombinases and either ZFa, we generate four defined setpoints from the nested DIAL promoter over a range spanning more than an order of magnitude (Fig 1H).

DIAL setpoints are robust to varying levels of ZFa

Cellular physiology and the process of gene expression contribute to variability in the expression of transgenes.[32–34] High variability in the expression of components can lead to poor performance of gene circuits.[29,35,36] Ideally, circuits can be designed to buffer variation and ensure robust performance across populations and over time.[5,37–41] For synthetic transcription factor systems, low expression of transcription factors contributes to bimodality, which is often masked by observation of only the mean level of the population (Fig 2A, B).[29] As bimodality contributes to poor control and circuit performance, promoter systems ideally generate unimodal expression of transgenes.

Potentially, sufficient expression of transactivators can establish regimes that are dosage-insensitive to transactivator levels. To examine the sensitivity of DIAL to variation in the levels of ZFa, we performed a titration of two ZFas (Fig 2B-C, Fig S7A-D). Using fluorescence markers for each ZFa, we measured the circuit input (ZFa) and the output (mGL expression) for the 203-bp DIAL promoter (Fig S8). At high levels of ZFa, the mean expression from the DIAL promoter remained constant at the induced setpoint (Fig 2D). In this dosage-invariant regime, the DIAL setpoints are maintained even while the level of ZFa ranges over one order of magnitude (Fig 2D). At lower ZF levels, bimodality emerges. The increasing population of cells in the “OFF” state increases causing the population means to decrease (Fig 2D). Isolating the cells expressing the output gene, we find that DIAL expression is invariant to levels of ZFa for both the high and the low setpoints (Fig 2E, Fig S2E). At lower ZFa levels, the fraction of reporter positive cells changes but the mean of the positive cells remains unchanged (Fig S2E).

We fit the data to simple model of transcription factor binding and transcription initiation using the ZFa plasmid titration curves (Fig S7I. Our model predicts that ZFa binding rate does not change upon editing. In comparison, reducing the distance between the activator binding sites and the minimal promoter increases the putative rate of transcriptional machinery recruitment, k_{cat}, 20-fold for ZF37-VP16 and 5-fold for ZF43-VP16 (Fig S7J).

We predicted that in addition to being robust to plasmid copy number, DIAL setpoints should be unaffected by the choice of the promoter controlling expression of ZFa. We generated a range of ZFa expression using constitutive promoters of different strengths (Fig 2F, Fig S7F-H). Consistent with the plasmid titration, setpoints in DIAL expression were uniform across the range of ZFa for both ZF37-VP16 and ZF43-VP16 and matched our model’s predictions (Fig 2G, Fig S2G). Together, this data demonstrates that titrating ZFa levels alters the fraction of cells expressing the output at a single setpoint. In contrast, DIAL allows for setting multiple output expression levels at a given ZFa input level in the

dosage-invariant regime. DIAL supports programmable, highly robust, and predictable unimodal setpoints.

DIAL transmits transient inputs into heritable states

Transmitting transient events into heritable states supports diverging cellular trajectories and event recording.[42–45] As editing of the DIAL promoter is recorded in the DNA, these states can be transiently induced and inherited, allowing cells to generate long-term trajectories from a temporally-defined stimulus (Fig 3A).

While plasmid transfection of recombinases works well in model cell lines, modRNA offers a simple method for transient *in vitro* and *in vivo* delivery of recombinases to diverse cell types.[46–48] We verified that modRNA encoding the Cre recombinase increases expression in a fraction of cells containing DIAL (Fig S9A). To examine the heritability of DIAL states, we delivered the DIAL promoter and ZFa on lentiviruses to HEK293T cells (Fig 3B). By co-delivering mRNA encoding Cre as well as a fluorescent marker (TagBFP), we estimate dilution of modRNA-delivered Cre over serial passaging (Fig 3C). TagBFP levels reach background expression by 9 days post transfection (dpt).

We observe that DIAL expression is heritable over this period, with a clear separation between the edited and unedited populations (Fig 3D). However, the mean expression of the edited population does decrease with time. We suspect that the decrease in mean expression results from expansion of unedited cells putatively resulting from inefficient editing from modRNA delivery of Cre. Higher expression of transgenes can induce cellular burden and reduce proliferation.[49,50] As expected if unedited cells expand, we see an increase in the fraction of cells at the lower peak, corresponding to the expression level of the unedited cells) (Fig 3E). Together, these data suggest that DIAL can induce heritable expression changes that can be tracked over multiple rounds of division. Additionally, the dose-dependent burden imposed by the fluorescent protein, suggests that DIAL may support identification of transgenes with subtle effects on proliferation.

Small-molecule control of Cre activity supports *in vivo* applications where stable integration of reporter and recombinase expression may be desirable. Cre-mediated editing can be induced via small-molecules and light.[51] Addition of gibberellin (GIB) induces Cre activity via chemical-inducible dimerization (CID) domains tethered to halves of the split Cre recombinase (Fig 3F).[51] In transfection, addition of GIB increased expression of the reporter over the uninduced state in the presence of ZFa (Fig 3F, S9D).

DIAL relies on expression of the ZFa. Thus, inducible, pathway-responsive, and cell-type specific promoters that regulate ZFa expression provide an additional method to selectively activate DIAL. To demonstrate that promoter-mediated control of the transactivator can layer control in DIAL, we encoded ZF37-VP16 under the DOX-inducible TRE3G promoter. As expected, combinations of DOX and Cre generate three setpoints of expression (Fig 3F, S9E-F). In summary, regulation of Cre and ZFa expression enable user-defined timing for change in setpoint from the same DIAL construct.

TET-DIAL system enables small-molecule activation of defined setpoints

We hypothesized that the DIAL framework would support expansion to other transactivator systems that rely on binding sites upstream of a core promoter. The commonly used TET system enables reversible, small molecule-based induction of transgenes. In the presence of doxycycline (DOX), the transactivator rtTA binds to the tet-responsive promoter composed of an array of tetO sites upstream of a minimal promoter, resulting in the expression of the downstream gene.

We hypothesized that incorporating the Tet system into the DIAL framework could shift expression unimodally between defined setpoints while maintaining reversible, small molecule-responsive induction. We constructed TET-DIAL by inserting a floxed spacer in between the tetO sites and the minimal CMV promoter (Fig 4A-B). Across a range of spacer lengths, addition of Cre increased output expression up to five-fold over pre-excision levels (Fig 4C-E, Fig S10A). The post-excision expression matched that of a control lacking a spacer, and we confirmed excision via PCR (Fig S10).

In the zinc-finger-based DIAL systems, we observed a bimodal output expression regime and a dosage-invariant regime as ZFa levels changed. In TET-DIAL, we observed similar behavior in output expression as rtTA levels changed (Fig 4C, Fig S10B). This suggests that properties of DIAL are generalizable across transactivators. Additionally, we performed a DOX titration for TET-DIAL. We found that as DOX concentration concurrently changes the mean expression and the fraction of the reporter expressing cells (Fig 4F, Fig 4G, Fig 4H, Fig S10C). As expected, in the presence of Cre, increasing DOX directs cells along a higher and steeper output expression profile (Fig 4H). Similar to our observation with ZFas, titrating the levels of the rTta also generated bimodal behavior in output expression (Fig S11). Putatively, DOX removal could then reversibly revert expression back to the “OFF” setpoint, supporting temporally induced control. Together, TET-DIAL enables unimodal shifts in output setpoint in the presence of adequate rtTA and high DOX while retaining the reversibility and temporal control offered by small-molecule induction.

DIAL is extensible across cell types and target genes

For broadest impact across research and therapeutics, genetic control systems such as DIAL need to perform in primary cells and human iPSCs. To examine how DIAL performs in primary cells, we delivered the DIAL promoter via lentivirus into mouse embryonic fibroblasts (MEFs) with combinations of ZFa and Cre (Fig 5A). As in HEK293Ts, addition of Cre increased expression with two different ZFa and at two different spacer lengths (Fig 5B). Addition of Cre did not change expression of the ZFa (Fig 5SA-B). As expected, the longer spacer reduced the pre-excision setpoint and led to a larger fold change in expression (Fig 5B-C, Fig 5SC-D). The stronger ZFa induced a larger range in output levels, visible by microscopy (Fig 5B). For temporal control of output expression in primary cells, the ZFa can be expressed from a lentiviral-delivered DOX-inducible TRE3G promoter with co-delivered rtTA (Fig 5E). Addition of

DOX induces expression of the ZFa which activates expression of the output gene. Viral delivery of Cre increases reporter expression (Fig 5F). DOX induced ZFa expression, which remained stable after Cre addition (Fig S5F). Transfecting DIAL in iPSCs, addition of Cre increased the reporter expression while the expression of a spacer-less control and the ZFa remained constant (Fig 5G-H, Fig S5F). Together, these results demonstrate DIAL is a general framework that performs across a range of cell types.

To execute titrations, enable screening, and enact diverse control functions, genetic controllers should be able to regulate arbitrary genes. To demonstrate that DIAL can control expression of functionally relevant genes, we replaced the fluorescent protein regulated by our DIAL promoter with transgenes encoding a tumor suppressor protein and an oncogene. To visualize expression and measure setpoints, we fused fluorescent reporters to each protein. Specifically, we fused *Trp53* to Halo, a ligand-labelable fluorescent protein, and the oncogene *HRASG12V* to mCherry. As expected, DIAL generates unimodal setpoints of expression of the fusion proteins Halo-p53 and mCherry-HRasG12V (Fig 5J-I, Fig S5G). Further, DIAL can regulate multiple genes expressed from polycistronic cassettes (Fig 5K). In summary, DIAL generates setpoints of expression for arbitrary genes and performs in primary cells and therapeutically-relevant cell types, supporting both research and translational applications.

Discussion

In this work, we present DIAL, a highly modular and extensible framework for engineering synthetic promoter systems. DIAL generates multiple unimodal setpoints of expression from a single promoter sequence (Fig 1). Using the DIAL framework, we generate a toolkit of promoters responsive to diverse synthetic transcription factors with rationally tunable setpoints and ranges. We demonstrate that recombinase-mediated editing of the DIAL promoter increases the setpoint of the target gene. DIAL can translate transient user-defined input in heritable changes in the setpoint, supporting flexibility in temporally changing setpoints. For broad application, we show that DIAL can regulate physiologically-relevant transgenes and performs across diverse cell types including human iPSC and primary murine cells.

Titrating the levels of synthetic transcription factors, we find that DIAL setpoints are robust to variation in the expression of the synthetic transcription factor (Fig 2). Over a ten-fold range of transcription factor expression, DIAL output remains constant. Precise programming of gene expression levels represents one of the most important and challenging goals in synthetic biology.[52–55] While tools for this control in mammalian systems have expanded over the last decade, few simple circuits have been translated clinically.[54] In part, these limitations are driven by poor performance in primary cells and emergent behaviors such as bimodality and transgene silencing.[29,35,36] DIAL offers unimodal expression at programmable setpoints. The combination of unimodality and dosage-invariance to component variation indicates that DIAL will improve the predictability and performance of gene circuits.

DIAL offers a highly modular and extensible framework for engineering synthetic promoters. In TET-DIAL, we demonstrate the extensibility of the DIAL framework to the doxycycline-inducible system, supporting reversible, small-molecule responsive induction (Fig 4). As the field has developed an array of synthetic promoter systems[10,56], we envision that the DIAL framework could guide design of multiple unimodal setpoints of expression in these systems. Similarly, integration of arrays of binding sites for diverse endogenous transcription factors into the DIAL framework may support tuning of cell-state responsive promoters.[28] Our toolkit uses two core promoter sequences. Exchanging these sequences for other core promoters of different types may further tune DIAL output and range.[57,58] Additionally, encoding pathway-responsive and tissue-specific promoters into DIAL may allow tuning of activity from these promoters and support circuits for information processing, recording, and computation of native signals.[25,59]

Our results highlight how transcription factor titration does not translate to titration of mean levels of output. Small-molecule titration of the doxycycline-inducible system slightly tunes mean, but comes at the expense of changing the fraction of cells that express the output gene. In developing DIAL, we have articulated a framework for robustly setting programmable expression levels in dosage insensitive regions. Via promoter editing, DIAL supports independent tuning of the mean levels and fractions of reporter-positive cells, which are otherwise coupled. As contact between promoters and enhancers provide one mode of native gene regulation, it is interesting to speculate how DIAL might be used to study transcriptional dynamics.[60] Potentially, decreasing the distance between the binding sites and core promoter increases the frequency of transcriptional bursts as has been observed for forced enhancer looping and other synthetic transcription factor systems.[61,62]

By nesting recombinase sites within the spacer, we expanded the number of DIAL setpoints (Fig 1). For independent control of setpoints for separate genes, DIAL requires orthogonal sets of recombinases. As more recombinases are being discovered and characterized[63], we expect that DIAL can expand to independent control of multiple genes for complex circuits. We show that Cre activity can be instigated by orthogonal control systems, including external user-defined cues opening opportunities to additional methods of tuning recombinase activity.[51,64] While recombinase systems have been used extensively for inducing expression, these system primarily control binary states of expression (ON/OFF).[43,51,65] In yeast, GEMbLER supports diversification of promoter sequences and expression profiles through random recombination of arrays of floxed endogenous promoters.[66] While such promoter recombination supports the identification of novel promoter combinations, random recombination does not support precise programming. Thus, DIAL's ability to provide fine-scale tuning offers a novel application for tyrosine recombinases. DIAL can potentially integrate into the abundance of recombinase-based tools for lineage tracing to allow increase the setpoint of transgenes at specific developmental windows and within specific subpopulations.[67–71]

While DIAL provides a number of features and insights into gene regulation, there remain limitations and opportunities to expand the capabilities. At high expression of the synthetic transcription factor, DIAL outputs do not change. However, other factors such as the dosage of the DIAL promoter itself may influence outputs. Alternative types of genetic controllers may provide control for variation in DNA dosage.[41,52,53,72,73] In its current form, DIAL allows us to increase but not decrease the level of the setpoint, limiting application to systems where a reduction in the setpoint level is needed. Although permanent editing is desirable for stability, it also means the increased setpoint levels cannot be reversed. TET-DIAL overcomes this limitation since removal of DOX allows cells to return to the OFF state but comes at the cost of requiring constant delivery of the small-molecule activator for sustained induction. We observed small changes in expression in changing transactivators and limited range of spacer length to extend the dynamic range of DIAL. While many applications require fine-scale changes of transgene expression, the lack of larger ranges may be a limitation. In the current form of DIAL, we selected spacer sequences which we rationally identified as putatively neutral. A more expansive characterization may identify sequence requirements for optimal performance of DIAL promoters.

DIAL expands the mammalian cell engineering toolkit to achieve precisely programmable profiles of gene expression. With ZFa and TET binding sites, we offer a set of DIAL promoters with a variety of fold changes and expression setpoints. We anticipate that the extensible framework offered by DIAL will support expansion to novel synthetic promoter systems and broadly improve precision cell engineering. By setting stable and heritable setpoints, DIAL provides a tool to investigate how transgene levels map to phenotypes which can support fundamental research in mechanisms related to development and oncogenesis.

References

1. Domingo, J. *et al.* Non-linear transcriptional responses to gradual modulation of transcription factor dosage. 2024.03.01.582837 Preprint at https://doi.org/10.1101/2024.03.01.582837 (2024).
2. Wang, N. B. *et al.* Proliferation history and transcription factor levels drive direct conversion. 2023.11.26.568736 Preprint at https://doi.org/10.1101/2023.11.26.568736 (2023).
3. Kueh, H. Y. *et al.* Positive feedback between PU.1 and the cell cycle controls myeloid differentiation. *Science* **341**, 670–673 (2013).
4. Desai, R. V. *et al.* A DNA-repair pathway can affect transcriptional noise to promote cell fate transitions. *Science* **373**, eabc6506 (2021).
5. Galloway, K. E., Franco, E. & Smolke, C. D. Dynamically Reshaping Signaling Networks to Program Cell Fate via Genetic Controllers. *Science* **341**, (2013).

6. Chen, J.-Y. *et al.* Multi range ERK responses shape the proliferative trajectory of single cells following oncogene induced senescence. 2022.10.06.511142 Preprint at https://doi.org/10.1101/2022.10.06.511142 (2022).
7. Takahashi, K. & Yamanaka, S. Induction of Pluripotent Stem Cells from Mouse Embryonic and Adult Fibroblast Cultures by Defined Factors. *Cell* **126**, 663–676 (2006).
8. Hong, M., Clubb, J. D. & Chen, Y. Y. Engineering CAR-T Cells for Next-Generation Cancer Therapy. *Cancer Cell* **38**, 473–488 (2020).
9. Goglia, A. G. *et al.* A Live-Cell Screen for Altered Erk Dynamics Reveals Principles of Proliferative Control. *Cell Systems* **10**, 240-253.e6 (2020).
10. Li, H.-S. *et al.* Multidimensional control of therapeutic human cell function with synthetic gene circuits. *Science* **378**, 1227–1234 (2022).
11. Collins, R. L. *et al.* A cross-disorder dosage sensitivity map of the human genome. *Cell* **185**, 3041-3055.e25 (2022).
12. Arita, Y. *et al.* A genome-scale yeast library with inducible expression of individual genes. *Mol Syst Biol* **17**, e10207 (2021).
13. Chapman, S. A. & Asthagiri, A. R. Quantitative effect of scaffold abundance on signal propagation. *Molecular Systems Biology* **5**, 313 (2009).
14. Legut, M. *et al.* A genome-scale screen for synthetic drivers of T cell proliferation. *Nature* **603**, 728–735 (2022).
15. Eguchi, A. *et al.* Reprogramming cell fate with a genome-scale library of artificial transcription factors. *Proc. Natl. Acad. Sci. U.S.A.* **113**, E8257–E8266 (2016).
16. Veerapandian, V. *et al.* Directed Evolution of Reprogramming Factors by Cell Selection and Sequencing. *Stem Cell Reports* **11**, 593–606 (2018).
17. Joung, J. *et al.* A transcription factor atlas of directed differentiation. *Cell* **186**, 209-229.e26 (2023).
18. Gao, X. J., Chong, L. S., Kim, M. S. & Elowitz, M. B. Programmable protein circuits in living cells. *Science* **361**, 1252–1258 (2018).

19. Zhu, R., del Rio-Salgado, J. M., Garcia-Ojalvo, J. & Elowitz, M. B. Synthetic multistability in mammalian cells. *Science* **375**, eabg9765 (2022).

20. Elowitz, M. B. & Leibler, S. A synthetic oscillatory network of transcriptional regulators. *Nature* **403**, 335–338 (2000).

21. Gardner, T. S., Cantor, C. R. & Collins, J. J. Construction of a genetic toggle switch in Escherichia coli. *Nature* **403**, 339–342 (2000).

22. Danino, T., Mondragón-Palomino, O., Tsimring, L. & Hasty, J. A synchronized quorum of genetic clocks. *Nature* **463**, 326–330 (2010).

23. Tabor, J. J. *et al.* A Synthetic Genetic Edge Detection Program. *Cell* **137**, 1272–1281 (2009).

24. Bashor, C. J., Helman, N. C., Yan, S. & Lim, W. A. Using Engineered Scaffold Interactions to Reshape MAP Kinase Pathway Signaling Dynamics. *Science* **319**, 1539–1543 (2008).

25. Ravindran, P. T., McFann, S., Thornton, R. H. & Toettcher, J. E. A synthetic gene circuit for imaging-free detection of signaling pulses. *Cell Systems* **13**, 131-142.e13 (2022).

26. Khalil, A. S. *et al.* A Synthetic Biology Framework for Programming Eukaryotic Transcription Functions. *Cell* **150**, 647–658 (2012).

27. Donahue, P. S. *et al.* The COMET toolkit for composing customizable genetic programs in mammalian cells. *Nat Commun* **11**, 779 (2020).

28. Wu, M.-R. *et al.* A high-throughput screening and computation platform for identifying synthetic promoters with enhanced cell-state specificity (SPECS). *Nature Communications* **10**, 2880 (2019).

29. Duran, A. G. *et al.* Limiting Transactivator Amounts Contribute to Transgene Mosaicism in Tet-On All-in-One Systems. *ACS Synth. Biol.* **11**, 2623–2635 (2022).

30. Randolph, L. N., Bao, X., Zhou, C. & Lian, X. An all-in-one, Tet-On 3G inducible PiggyBac system for human pluripotent stem cells and derivatives. *Sci Rep* **7**, 1549 (2017).

31. Nevozhay, D., Zal, T. & Balázsi, G. Transferring a synthetic gene circuit from yeast to mammalian cells. *Nat Commun* **4**, 1451 (2013).

32. Zopf, C. J., Quinn, K., Zeidman, J. & Maheshri, N. Cell-cycle dependence of transcription dominates noise in gene expression. *PLoS Comput Biol* **9**, e1003161 (2013).

33. Quarton, T. *et al.* Uncoupling gene expression noise along the central dogma using genome engineered human cell lines. *Nucleic Acids Res* **48**, 9406–9413 (2020).

34. Babos, K. N. *et al.* Mitigating Antagonism between Transcription and Proliferation Allows Near-Deterministic Cellular Reprogramming. *Cell Stem Cell* **25**, 486-500.e9 (2019).

35. Fitzgerald, M., Livingston, M., Gibbs, C. & Deans, T. L. Rosa26 docking sites for investigating genetic circuit silencing in stem cells. *Synthetic Biology* **5**, (2020).

36. Cabrera, A. *et al.* The sound of silence: Transgene silencing in mammalian cell engineering. *Cell Systems* **13**, 950–973 (2022).

37. Jones, R. D. *et al.* Robust and tunable signal processing in mammalian cells via engineered covalent modification cycles. *Nat Commun* **13**, 1720 (2022).

38. Frei, T., Chang, C.-H., Filo, M., Arampatzis, A. & Khammash, M. A genetic mammalian proportional–integral feedback control circuit for robust and precise gene regulation. *Proceedings of the National Academy of Sciences* **119**, e2122132119 (2022).

39. Johnstone, C. P. & Galloway, K. E. Supercoiling-mediated feedback rapidly couples and tunes transcription. *Cell Reports* **41**, (2022).

40. Lillacci, G., Benenson, Y. & Khammash, M. Synthetic control systems for high performance gene expression in mammalian cells. *Nucleic Acids Research* **46**, 9855–9863 (2018).

41. Strovas, T. J., Rosenberg, A. B., Kuypers, B. E., Muscat, R. A. & Seelig, G. MicroRNA-based single-gene circuits buffer protein synthesis rates against perturbations. *ACS Synth Biol* **3**, 324–331 (2014).

42. Askary, A. *et al.* In situ readout of DNA barcodes and single base edits facilitated by in vitro transcription. *Nature Biotechnology* **38**, 66–75 (2020).

43. Kim, T., Weinberg, B., Wong, W. & Lu, T. K. Scalable recombinase-based gene expression cascades. *Nat. Commun.* **12**, 2711 (2021).

44. Loveless, T. B. *et al.* Lineage tracing and analog recording in mammalian cells by single-site DNA writing. *Nat Chem Biol* **17**, 739–747 (2021).

45. Sheth, R. U. & Wang, H. H. DNA-based memory devices for recording cellular events. *Nat Rev Genet* **19**, 718–732 (2018).

46. Shi, D., Toyonaga, S. & Anderson, D. G. In Vivo RNA Delivery to Hematopoietic Stem and Progenitor Cells via Targeted Lipid Nanoparticles. *Nano Lett.* **23**, 2938–2944 (2023).

47. Sago, C. D. *et al.* High-throughput in vivo screen of functional mRNA delivery identifies nanoparticles for endothelial cell gene editing. *Proceedings of the National Academy of Sciences* **115**, E9944–E9952 (2018).

48. Blanch-Asensio, A. *et al.* STRAIGHT-IN enables high-throughput targeting of large DNA payloads in human pluripotent stem cells. *Cell Reports Methods* **2**, (2022).

49. Frei, T. *et al.* Characterization and mitigation of gene expression burden in mammalian cells. *Nat Commun* **11**, 4641 (2020).

50. Jones, R. D. *et al.* An endoribonuclease-based feedforward controller for decoupling resource-limited genetic modules in mammalian cells. *Nat Commun* **11**, 5690 (2020).

51. Weinberg, B. H. *et al.* High-performance chemical- and light-inducible recombinases in mammalian cells and mice. *Nat Commun* **10**, 4845 (2019).

52. Du, R., Flynn, M. J., Honsa, M., Jungmann, R. & Elowitz, M. B. miRNA circuit modules for precise, tunable control of gene expression. 2024.03.12.583048 Preprint at https://doi.org/10.1101/2024.03.12.583048 (2024).

53. Flynn, M. J., Mayfield, A. M., Du, R., Gradinaru, V. & Elowitz, M. B. Synthetic dosage-compensating miRNA circuits for quantitative gene therapy. 2024.03.13.584179 Preprint at https://doi.org/10.1101/2024.03.13.584179 (2024).

54. Bashor, C. J., Hilton, I. B., Bandukwala, H., Smith, D. M. & Veiseh, O. Engineering the next generation of cell-based therapeutics. *Nat Rev Drug Discov* **21**, 655–675 (2022).

55. O'Connell, R. W. *et al.* Ultra-high throughput mapping of genetic design space. 2023.03.16.532704 Preprint at https://doi.org/10.1101/2023.03.16.532704 (2023).

56. Tycko, J. *et al.* High-throughput discovery and characterization of human transcriptional effectors. 63.

57. Ede, C., Chen, X., Lin, M.-Y. & Chen, Y. Y. Quantitative Analyses of Core Promoters Enable Precise Engineering of Regulated Gene Expression in Mammalian Cells. *ACS Synth. Biol.* **5**, 395–404 (2016).

58. Hong, C. K. Y. & Cohen, B. A. Genomic environments scale the activities of diverse core promoters. *Genome Res.* **32**, 85–96 (2022).

59. Ravindran, P. T., Wilson, M. Z., Jena, S. G. & Toettcher, J. E. Engineering combinatorial and dynamic decoders using synthetic immediate-early genes. *Communications Biology* **3**, 1–10 (2020).

60. Johnstone, C. P., Wang, N. B., Sevier, S. A. & Galloway, K. E. Understanding and Engineering Chromatin as a Dynamical System across Length and Timescales. *Cell Systems* **11**, 424–448 (2020).

61. Bartman, C. R., Hsu, S. C., Hsiung, C. C.-S., Raj, A. & Blobel, G. A. Enhancer Regulation of Transcriptional Bursting Parameters Revealed by Forced Chromatin Looping. *Molecular Cell* **62**, 237–247 (2016).

62. Popp, A. P., Hettich, J. & Gebhardt, J. C. M. Altering transcription factor binding reveals comprehensive transcriptional kinetics of a basic gene. *Nucleic Acids Res.* **49**, 6249–6266 (2021).

63. Durrant, M. G. *et al.* Systematic discovery of recombinases for efficient integration of large DNA sequences into the human genome. *Nat Biotechnol* 1–12 (2022) doi:10.1038/s41587-022-01494-w.

64. Meador, K. *et al.* Achieving tight control of a photoactivatable Cre recombinase gene switch: new design strategies and functional characterization in mammalian cells and rodent. *Nucleic Acids Research* **47**, e97 (2019).

65. Weinberg, B. H. *et al.* Large-scale design of robust genetic circuits with multiple inputs and outputs for mammalian cells. *Nature Biotechnology* **35**, 453–462 (2017).

66. Cautereels, C. *et al.* Combinatorial optimization of gene expression through recombinase-mediated promoter and terminator shuffling in yeast. *Nat Commun* **15**, 1112 (2024).

67. Kretzschmar, K. & Watt, F. M. Lineage Tracing. *Cell* **148**, 33–45 (2012).

68. Yang, D. *et al.* Lineage tracing reveals the phylodynamics, plasticity, and paths of tumor evolution. *Cell* **185**, 1905-1923.e25 (2022).

69. Anderson, T. *et al.* Ligament injury in adult zebrafish triggers ECM remodeling and cell dedifferentiation for scar-free regeneration. *npj Regen Med* **8**, 1–15 (2023).

70. Nowak, J. A., Polak, L., Pasolli, H. A. & Fuchs, E. Hair Follicle Stem Cells Are Specified and Function in Early Skin Morphogenesis. *Cell Stem Cell* **3**, 33–43 (2008).

71. Le Bin, G. C. *et al.* Oct4 is required for lineage priming in the developing inner cell mass of the mouse blastocyst. *Development* **141**, 1001–1010 (2014).

72. Bleris, L. *et al.* Synthetic incoherent feedforward circuits show adaptation to the amount of their genetic template. *Mol Syst Biol* **7**, 519 (2011).

73. Yang, J. *et al.* A synthetic circuit for buffering gene dosage variation between individual mammalian cells. *Nat Commun* **12**, 4132 (2021).

ACKNOWLEDGEMENTS

Research reported in this manuscript was supported by the National Institute of General Medical Sciences of the National Institutes of Health under Health under award number R35-GM143033, by the National Science Foundation under the NSF-CAREER under award number 2339986, and the with funding from Institute for Collaborative Biotechnologies. S.R.K., B.A.L, and E.L.P are supported by the National Science Foundation Graduate Research Fellowship Program under grant No. 1745302. AMB is supported by the National Cancer Institute under award number F99CA284280. We thank the Koch Institute's RA. Swanson (1969) Biotechnology Center (National Cancer Institute Grant P30-CA14051) for technical support, specifically the Flow Cytometry Core Facility. We thank Christopher Johnstone, Joji Teves, Diya Godavarti, and Jane Atkinson for feedback on the development of the manuscript.

AUTHOR CONTRIBUTIONS

S.R.K., Y.B., and K.E.G. conceived and outlined the project. S.R.K., Y.B., M.E.E., and K.E.G. and analyzed DIAL and TET-DIAL characterization. A.M.B. and B.A.L. performed lenti delivery to primary mouse embryonic fibroblasts and analyzed data. E.L.P. and K.S.L. performed iPSC transfections. DP assisted with experimental design and production of modRNA. S.R.K., Y.B., M.E.E., A.M.B. and B.A.L., and K.E.G. wrote the manuscript. K.E.G. supervised the project.

DECLARATION OF INTERESTS

Patent applications related to this work have been filed by the Massachusetts Institute of Technology.

DATA AND MATERIALS AVAILABILITY

Data needed to evaluate the conclusions are available in the paper or the Supplementary Materials. Raw data and computer codes used for data analysis are available from the corresponding author.

Experimental Model and Subject Details

Cell lines and tissue culture

HEK293T, Plat-E, and mouse embryonic fibroblasts were cultured using DMEM (Genesee Scientific 25-500) + 10% FBS (Genesee Scientific 25-514H) and incubated at 37C with 5% CO2. Plat-E cells were selected using 10 µg/mL blastocidin and 1 µg/mL puromycin every three passages. HEK293T, Plate-E, and mouse embryonic fibroblasts were detached from flasks using Trypsin (Genesee Scientific 25-510) diluted in PBS. For seeding and passaging, cells were counted using a hemocytometer. Cells were periodically tested for mycoplasma.

iPSC cell culture

IPS11 cells were cultured using mTeSR™ Plus (STEMCELL Technologies, 100-1130) with Geltrex™ (ThermoFisher Scientific, A1413302) coating and incubated at 37C with 5% CO2. For passaging, iPS11 cells were dissociated in clumps using ReLeSR™ (STEMCELL Technologies, 100-0484) according to the manufacturer's instructions. For experiments, iPS11 cells were dissociated into single cells using Gentle Cell Dissociation Reagent (STEMCELL Technologies, 100-1077), counted using a hemocytometer, and replated in mTeSR™ Plus with ROCK inhibitor (Millipore Sigma, Y0503-5MG) and Penicillin-Streptomycin (ThermoFisher Scientific, 10-378-016).

MEF dissection and isolation
C57BL/6 mice were mated with mice bearing the Hb9::GFP reporter. Mouse embryonic fibroblasts were isolated at E12.5-E14.5 under a dissection microscope. Embryos were sorted into non-transgenic and Hb9::GFP+ by using a blue laser to illuminate the spinal cord to identify the presence of Hb9::GFP+ cells. After removing the head and internal organs to avoid contaminating neurons and other cells, razors were used to break up the tissue for 5 minutes in the presence of 0.25% Trypsin-EDTA. Up to two embryos were processed at the same time. The preliminary suspension was neutralized, resuspended, and triturated with 0.25% Trypsin-EDTA. The suspension was neutralized and resuspended again before filtering through a 40 µm cell strainer. MEF cultures were expanded on 10 cm dishes coated with 0.1% gelatin, using one 10 cm dish per embryo. MEFs were expanded until ~80% confluent, passaged, and expanded for at least 3-4 days. Passage 1 MEFs were tested for mycoplasma, cryopreserved in 90% FBS and 10% DMSO, and stored in liquid nitrogen.

Method Details

Plasmid Cloning
Plasmids were cloned using standard cloning protocols for Gibson assembly and Golden Gate assembly. Promoters, target genes, and polyA signals were inserted into part position vectors (pPVs) via Gibson assembly. Expression plasmids were assembled via BsaI (New England Biolabs) Golden Gate Assembly using pPVs or Q5 polymerase-amplified and gel-purified DNA fragments. The lentivirus or retrovirus plasmids were assembled with PaqCI Golden Gate Assembly using expression plasmids and viral backbone plasmids.

DIAL promoter cloning
The DIAL promoter was constructed by inserting a spacer sequence between loxP or VloxP sites. The spacer is a tandem sequence of two putatively neutral regions of an expression plasmid, joined by restriction digest and Gibson assembly. The loxP and VloxP sequences were taken from respective recombinase reporters (gifts from the Wong Lab at Boston University, BW338 and BW273). Tessellated ZF43/37 hybrid binding sites were taken from ZF reporter Addgene plasmids #138934. The DIAL promoter was assembled through Golden Gate or Gibson assembly, using PCR products of spacer sequence and ZF binding sites with complementary overhangs. Additional recombinase binding sites were inserted using Gibson assembly with PCR overhangs. The assembled DIAL promoters were inserted into pPVs to produce downstream gene constructs through Golden Gate assembly.

Recombinase and Zinc Finger Activator Plasmids
Unless otherwise specified, in transient transfections, recombinase was expressed as: Cre from CAG-Cre-RbG (Addgene plasmid #89573), VCre from CAG-VCre-RbG (Addgene plasmid #89575), GIB-Cre N-terminal (Addgene plasmid #108723), and GIB-Cre C-terminal (Addgene plasmid #108724) (gifts from the Wong Lab at Boston University). Unless otherwise specified, zinc finger activators (ZFa) were expressed from EF1a-VP16-ZF37-2A-mCherry, EF1a-VP16-ZF43-2A-TagBFP, CMV-VP64-ZF37-BGH (Addgene plasmid #138834), CMV-VP64-ZF43-BGH (Addgene plasmid #138835), and CMV-VPR-ZF37-BGH (Addgene plasmid #138839). PCR fragments of Addgene plasmids #138759 and #138730 were used to clone target gene pPVs for VP16-ZF37 and VP16-ZF43 through Gibson assembly. The 2A-tagged ZFs were subsequently inserted into expression vectors with EF1a and BGH polyA signal via Golden Gate assembly with BsaI (NEB Stable).

HEK293T DNA Transient Transfection
39,000-42,000 cells were plated per well in a 96-well plate 24 hours before transfection. Cells were transfected on day 0 with 112.5 ng/plasmid/well delivered via a 4:1 ratio of ug PEI to ug of DNA mixed in

KnockOut DMEM (Fisher Scientific, 10-829-018). Unless specified, each well was transfected with 112 ng of all plasmids except the recombinase plasmid, which was transfected with 11 ng per well. All transfection experiments included a co-transfection marker EF1a-iRFP670-BGH (112 ng). Also, all transfection experiments had the same total DNA and PEI per condition within the experiment by using an empty vector plasmid to keep the total ug of DNA per well consistent. At 1 day post-transfection (dpt), media was aspirated and replaced with DMEM + 10% FBS. As specified, in some experiments, this replacement media at 1 dpt contained 1x DOX (1 ug/mL, from 1000X stock of 1 mg/mL stored at -20C or 4C) and appropriately titrated down conditions or 1x gibberellin (G3-AM, Sigma Aldrich, from 1000X stock of 10 mM dissolved in ethanol and stored at -20 C). For applicable experiments, modRNA was also transfected at 1 dpt. Cells were flowed and imaged at 3 dpt in technical triplicates. Bioreplicates represent separate transfection experiments. To detach cells from wells in preparation for flow cytometry, 1:1 Trypsin/1xPBS mixture was added to each well. After 8 minutes, DMEM + 10% FBS was added on top before centrifuging down the plates at 1000 rpm for 10 minutes. Media was aspirated and cells were resuspended in 1x PBS to transfer to a round bottom plate for flow cytometry. All experiments were conducted with at least biological replicates (n=3).

HEK293T Cell Line Development and Experiment

HEK293T cells were infected with lentivirus containing ZFa cassette EF1a-VP16-ZF37-2A-mCherry-BGH and reporter lentiviruses of 203 bp spacer DIAL promoter with mGL-WPRE, with and without divergent EF1a-iRFP670-BGH. At 3 dpt, cells were passaged into a 6-well plate. At 10 dpt, cells positive for iRFP670 (if present in reporter cassette) and mGL were sorted using a Sony MA900. Cells were cultured in a 24-well plate until confluent. 20,000 cells in triplicates were then plated into 96-wells. One population of cells in triplicate were delivered with 100 ng of TagBFP modRNA and 100 ng of Cre modRNA. Cells were flowed and passaged 1:5 at 3 dpt and 6 dpt. Cells were flowed once more at 9 dpt. Flow data was gated for both mGL and mCherry for analysis.

iPSC Transient Transfection Experiments

15,000 iPS11 cells were plated per well in a 96-well plate 48 hours before transfection. 24 hours before transfection, media containing ROCK inhibitor was removed and replaced with mTeSR™ Plus with Penicillin-Streptomycin. On the day of transfection, the media was changed to Opti-MEM™ (ThermoFisher Scientific, 31985062) and transfection mixes were prepared with FUGENE® HD (FuGENE, HD-1000) according to the manufacturer's instructions (ratio of 3 uL reagent to 1 ug DNA). Each well was transfected with 100 ng plasmid reporter, 12.5 ng zinc finger plasmid, 25 ng Cre plasmid, and 25 ng transfection marker plasmid. At 4 hours after transfection, mTeSR™ Plus with Penicillin-Streptomycin was added. At 24 hours after transfection, the media was changed to mTeSR™ Plus with Penicillin-Streptomycin. Cells were flowed at 2 DPT and imaged at both 1 DPT and 2 DPT in technical triplicates. To flow, cells were detached from wells using Gentle Cell Dissocation Reagent (STEMCELL Technologies, 100-1077) for 8 minutes and centrifuged at 500g for 5 minutes. Media was aspirated and cells were resuspended in 1x PBS and transferred to a round bottom plate for flow cytometry.

PCR of Cell Lysis

DNA from transfected HEK293Ts was obtained with Cell Lysis Buffer (10X) (Cell Signaling Technology 9803S). Cells were detached from wells using a 1:1 Trypsin/1x PBS mixture for 8 minutes. DMEM + 10% FBS was added on top and plates were centrifuged down at 1000 rpm for 10 minutes. Media was aspirated and cells were resuspended in 50 uL Cell Lysis Buffer (10X) and 0.5 uL of Proteinase K (New England Biolabs P8107S) per 96-well. Cells were incubated for 45 minutes at 85 C then microfuged. 1 uL of the supernatant was used for PCR using Apex Taq RED Master Mix, 2X (Genesee Scientific 42-138B). PCR products were run on a 2% agarose gel at 110V for 45-60 minutes.

In vitro transcription and transfection of Cre modRNA.
The plasmid template used for Cre modRNA synthesis harbors the 5'-UTR of human β-globin, a Kozak sequence, the coding sequence for iCre, and the 3'-UTR of human β-globin. The linear template for *in vitro* transcription (IVT) was generated via PCR using Q5 DNA Polymerase (New England Biolabs) with the forward primer (5'- AGCTATAATACGACTCACTATAAGctcctgggcaacgtgctg-3') encoding the T7 promoter (upper-case bases) and binding the 5' UTR (lower-case bases) and the reverse primer (5'-poly$(T)_{116}$-GCAATGAAAATAAATGTTTTTTATTAGGCAGAAT-3') encoding the poly(A) tail and binding the 3'-UTR. The PCR product was isolated on a 1% agarose gel, excised, and purified using the Monarch PCR and DNA Cleanup Kit (New England Biolabs). 200 ng of purified product was used in a 20 µL IVT reaction using the HiScribe T7 High Yield RNA Synthesis Kit (New England Biolabs), fully substituting UTP with N1-methylpseudouridine-5'-phosphate (TriLink Biotechnologies) and co-transcriptionally capping with CleanCap Reagent AG (TriLink Biotechnologies). IVT reactions were incubated at 37 °C for 4 hr, at which point reactions were diluted to 50 µL, treated with 2 µL DNase I, and incubated at 37 °C for 30 min to degrade the IVT PCR template DNA. Synthesized modRNA was column purified and eluted with 60 µL water using the 50 µg Monarch RNA Cleanup Kit (New England Biolabs). A small sample was nanodropped and ran on a native denaturing gel to determine RNA concentration and verify full-length product. The modRNA was dispensed in single-use aliquots and stored at –80 °C. For Cre modRNA transfection experiments, each 96-well was transfected with 200 ng of modRNA using 0.4 µL Lipofectamine MessengerMAX (Thermo Fisher Scientific) according to manufacturer's instructions.

Retrovirus production in Plat-Es
Plat-E cells were seeded at 850k per 6-well onto plates coated with 0.1% gelatin. The next day, Plat-Es were transfected with 1.8 µg of DNA per well using a 4:1 ratio of µg PEI:µg DNA. The next day, the media was replaced with 1.25 mL fresh 25 mM HEPES buffered DMEM with 10% FBS. The next day, viral supernatant was collected and filtered through a 0.45 µm filter. 1.25 mL fresh media was again added to the Plat-E cells. Filtered viral supernatant was then used for transduction of MEFs. Viral supernatant collection, filtration, and transduction was repeated for a second day. One day after the second viral transduction was considered one day post infection (dpi).

Lentiviral production in HEK293Ts
HEK293T cells were seeded at 1 million per 6-well onto plates coated with 0.1% gelatin. The next day, each well of 293Ts was transfected with 1.02 µg packaging plasmid (psPax2), 2.05 µg of envelope plasmid (pMD2.G), and 1.02 µg of transfer plasmid using a 4:1 ratio of ug PEI:µg DNA. 6-8 hours later, the media was replaced with 1.25 mL of fresh 25 mM HEPES buffered DMEM with 10% FBS. 24 and 48 hours later viral supernatant was collected and stored at 4°C, replacing with fresh media after the first collection. After the second collection, the viral supernatant was filtered with a 0.45 µM filter and was mixed with 1 volume Lenti-X concentrator to 3 volumes viral supernatant and incubated at 4°C overnight. The virus was pelleted by centrifugation at 1,500 x g for 45 minutes at 4°C. The supernatant was removed, and the pellets were resuspended in media to a final volume of 33 µL per 6-well of virus. Volumes and cell numbers were scaled up proportionally for a 10-cm plate. Concentrated virus was resuspended to a final volume of 1 mL per 10-cm plate of virus. The virus was used for transduction of MEFs on the same day.

Viral transduction of mouse embryonic fibroblasts (MEFs)
MEFs were seeded one day prior to viral transduction onto plates coated with 0.1% gelatin at 10k per 96-well. MEFs were transduced two days in a row with 11 µL of each PlatE retrovirus per 96-well. On the second day MEFs were also transduced with 3 µL per 96-well of concentrated lentivirus from a 6-well plate, or 5 uL per 96-well of concentrated lentivirus from a 10-cm plate. Fresh media was included to reach a final volume of 100 µL per 96-well, and 5 ug/mL polybrene was added to increase transduction

efficiency. One the second day of transduction the plates were also centrifuged at 1500 x g for 90 minutes at 32°C to further increase lentiviral transduction efficiency. At 1 dpi the transduction media was replaced with fresh DMEM + 10% FBS. At 3 dpi, the cells were dissociated using trypsin and analyzed via flow cytometry.

Imaging.
Images were taken on Keyence™ All-in-one fluorescence microscope BZ-X800.

Flow cytometry data analysis.
Live cells were gated based of FSC-A and SSC-A using FlowJo. Subsequently, single cells were gated via SSC-H and SSC-A. Single cells were then exported all plots and statistics were generated from pandas and seaborn packages in Python. Cells were additionally gated by co-transfection marker, ZFa, or output positive cells as specified in figure captions. Gating by transfection marker is shown in Figure S2.

<u>Mathematical modeling of DIAL activity for varying levels of ZFa.</u>

Dose-dependent reporter gene activation via ZFa titration was modeled using the Hill equation.

$$\frac{d[Reporter_{RNA}]}{dt} = k_{cat}\frac{[ZF_{protein}]^n}{K_M + [ZF_{protein}]^n} + \alpha - \beta[Reporter_{RNA}]$$

The relationship between reporter gene transcription and translation was simplified to obtain
$\frac{d[Reporter_{protein}]}{dt} = k_{cat}\frac{[ZF_{protein}]^n}{K_M+[ZF_{protein}]^n} + \alpha - \beta[Reporter_{protein}]$

where $k_{cat}$is the translation rate constant; α is the leaky expression from TF-independent transcription; and β is the degradation constant.

Assuming steady state of cellular processes, the reporter protein levels are expressed as

$$[Reporter_{protein}] = \frac{k_{cat}}{\beta}\frac{[ZF_{protein}]^n}{K_M + [ZF_{protein}]^n} + \frac{\alpha}{\beta}$$

Experimental data from the ZFa was divided into conditions (e.g in the presence or absence of Cre) to generate separate parameters that captures the different gene regulation across pre- and post-excision constructs. Parameters k_{cat} and α consolidated to simplify the steady state equation as follows:

$$[Reporter_{protein}] = k'_{cat}\frac{[ZF_{protein}]^n}{K_M + [ZF_{protein}]^n} + \alpha'$$

The leakiness parameter α' was set to the lowest value of output mGL in each condition corresponding to no ZFa added. Assuming no Hill cooperativity for ZF binding ($n = 1$), the experimental data was used as $[ZF_{protein}]$ and $[Reporter_{protein}]$ to calculate parameters k'_{cat} and K_M from the equation.

To minimize technical variance, the ZFa titration data was normalized by the 0.125xZFa condition (14 ng per well) within each bioreplicate. Potentially due to resource burden at high DNA concentration of ZFa, expression of mGL decreased at the highest levels of input mCherry (ZF37). These datapoints were removed before generating parameters to prevent the predicted parameters from reflecting resource burden which is not incorporated in these model equations. The data was transformed by the leaky mCherry or TagBFP expression in conditions with no ZF to normalize 0x ZFa conditions to no input ZF expression levels.

To fit the model, the data was bootstrapped across each condition (e.g in the presence or absence of Cre). The level of protein expression from the DIAL promoter was used to calculate parameters and generate a corresponding predicted titration curve for each bootstrapped sample. The 95% confidence interval of the titration curve was generated by selecting the 2.5th and 97.5th percentile output mGL values for each input mCherry or TagBFP value.

ZF37 titration

Parameters	No Cre	Cre
k'_{cat}	0.99	15.63
K_M	0.21	0.52
α'	0.14	0.22

ZF43 titration

Parameters	No Cre	Cre
k'_{cat}	1.13	5.21
K_M	0.19	0.20
α'	0.08	0.08

Figures

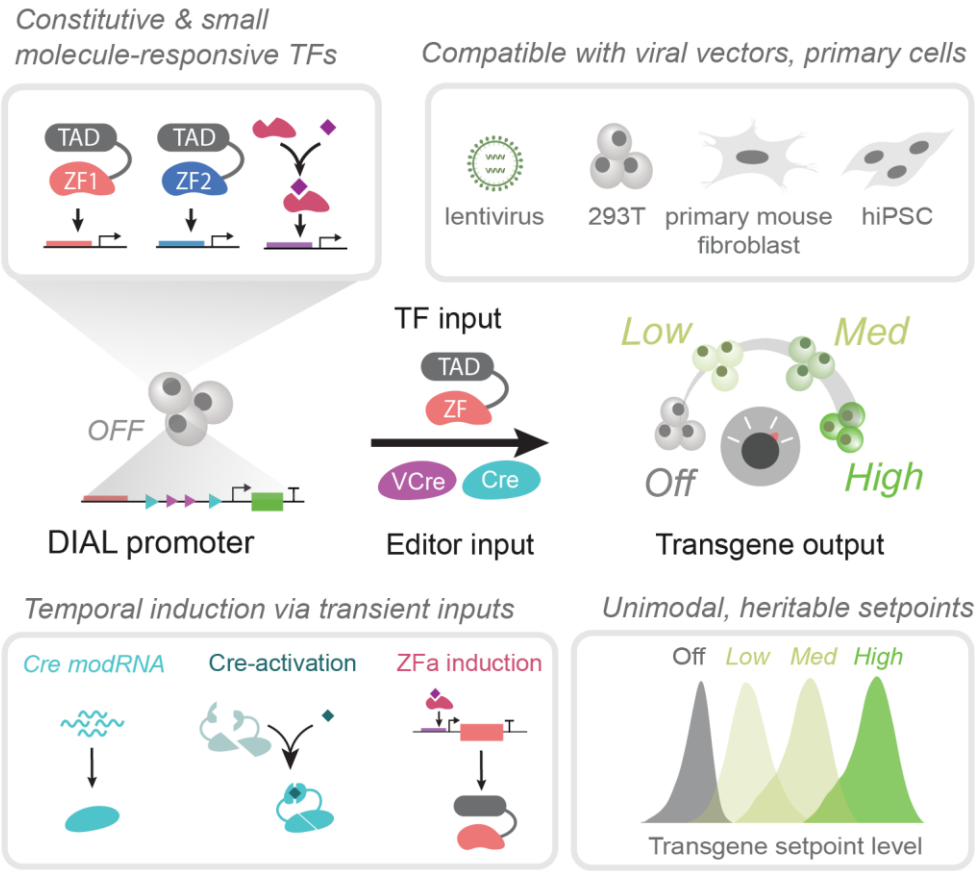

Overview

DIAL offers an extensible framework for designing synthetic promoters that generate heritable setpoints of gene expression and perform across a range of cell types and delivery systems.

Figure 1. Promoter editing generates a range of unimodal setpoints.

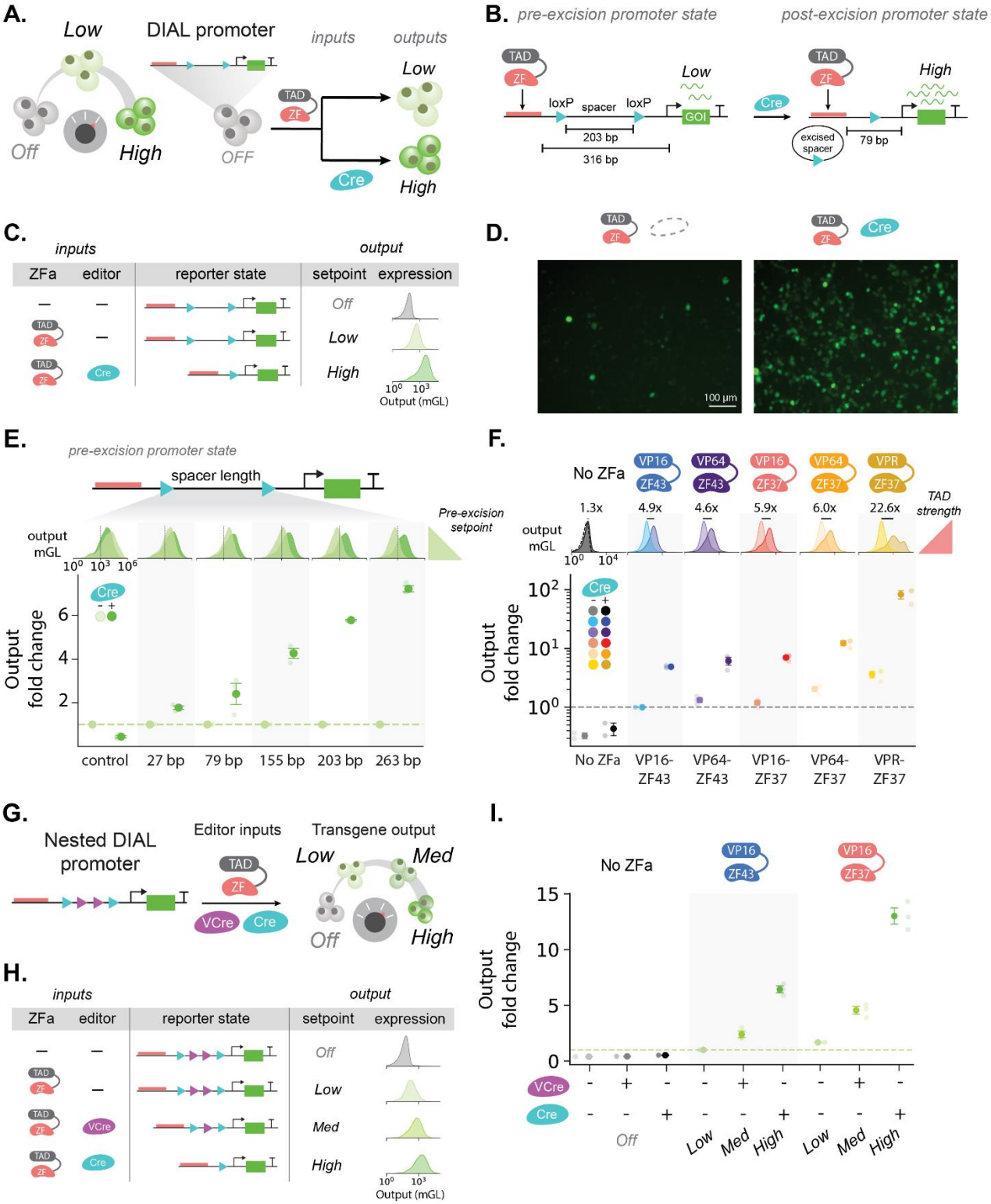

Figure 1. Promoter editing generates a range of unimodal setpoints.

(A) Schematic of the DIAL promoter system. DIAL uses combinatorial inputs to generate different setpoints of gene expression.
(B) Schematic of the molecular state of the DIAL promoter before and after Cre-mediated editing. The excision of the floxed 203 base pair (bp) spacer reduces the total distance between the ZF binding sites and YB_TATA minimal promoter from 316 bp to 79 bp, increasing expression.
(C) Logic table showcasing different input combinations of ZFa and Cre and corresponding output expected reporter state, target setpoint, and observed gene (mGL) expression from the DIAL promoter. Expression histograms show output increase upon addition of ZFa (VP16-ZF37) and Cre with the 203 bp spacer DIAL promoter regulating mGL.
(D) Fluorescence microscopy images 3 days post-transfection (dpt) of transfected HEK293T cells with VP16-ZF37 and 203 bp spacer DIAL promoter regulating mGL, with and without Cre.
(E) HEK293T transfection data with ZFa (VP16-ZF37) and DIAL promoters with different spacer lengths regulating mGL, in the presence or absence of Cre. Plots show fold change of output mGL geometric mean fluorescence intensity (MFI) normalized to the condition without Cre within each spacer length. Histograms show single cell distributions of output mGL, with vertical line at 1000 for ease of comparison across conditions. Increasing spacer length leads to lower pre-excision expression and an increasing shift between conditions with and without Cre.
(F) HEK293T transfection data with different zinc finger transactivation domains (different ZFa) and 203 bp spacer DIAL promoter regulating mGL, in the presence or absence of Cre. Plot shows fold change of output mGL geometric MFI normalized to the condition with VP16-ZF43 without Cre. Histograms show shift in output mGL between conditions with and without Cre for each ZFa. Plots and histograms of single-cell distributions of output mGL show fold change increases slightly with stronger ZFa.
(G) Schematic of a nested DIAL promoter with loxP (blue) and VloxP (purple) sites. Based on a combinatorial input of ZFa, VCre, and Cre, the nested DIAL promoter can achieve four different levels of transgene output.
(H) Logic table showcasing different input combinations of ZFa, VCre, and Cre and corresponding output reporter state, target setpoint, and observed gene (mGL) expression for the nested DIAL promoter. An additional setpoint is achieved compared to the logic table in (C).
(I) HEK293T transfection data without ZFa, with VP16-ZF43, or with VP16-ZF37 and nested DIAL promoter regulating mGL, in the presence or absence of Cre and VCre. Plot shows fold change of output mGL geometric MFI normalized to the condition with VP16-ZF43 without Cre and VCre.

All units for output MFI are a.u., and fold change is unitless. Large points in summary plots represent mean of biological replicates -/+ standard error. Histograms represent single-cell distributions sampled across bioreplicates (n=3). Statistical significance was calculated with Students t-Test with ns $p>0.05$; *$p<0.05$; **$p<0.01$; *** $p<0.001$.

Figure 2. DIAL setpoints are robust to varying levels of ZFa.

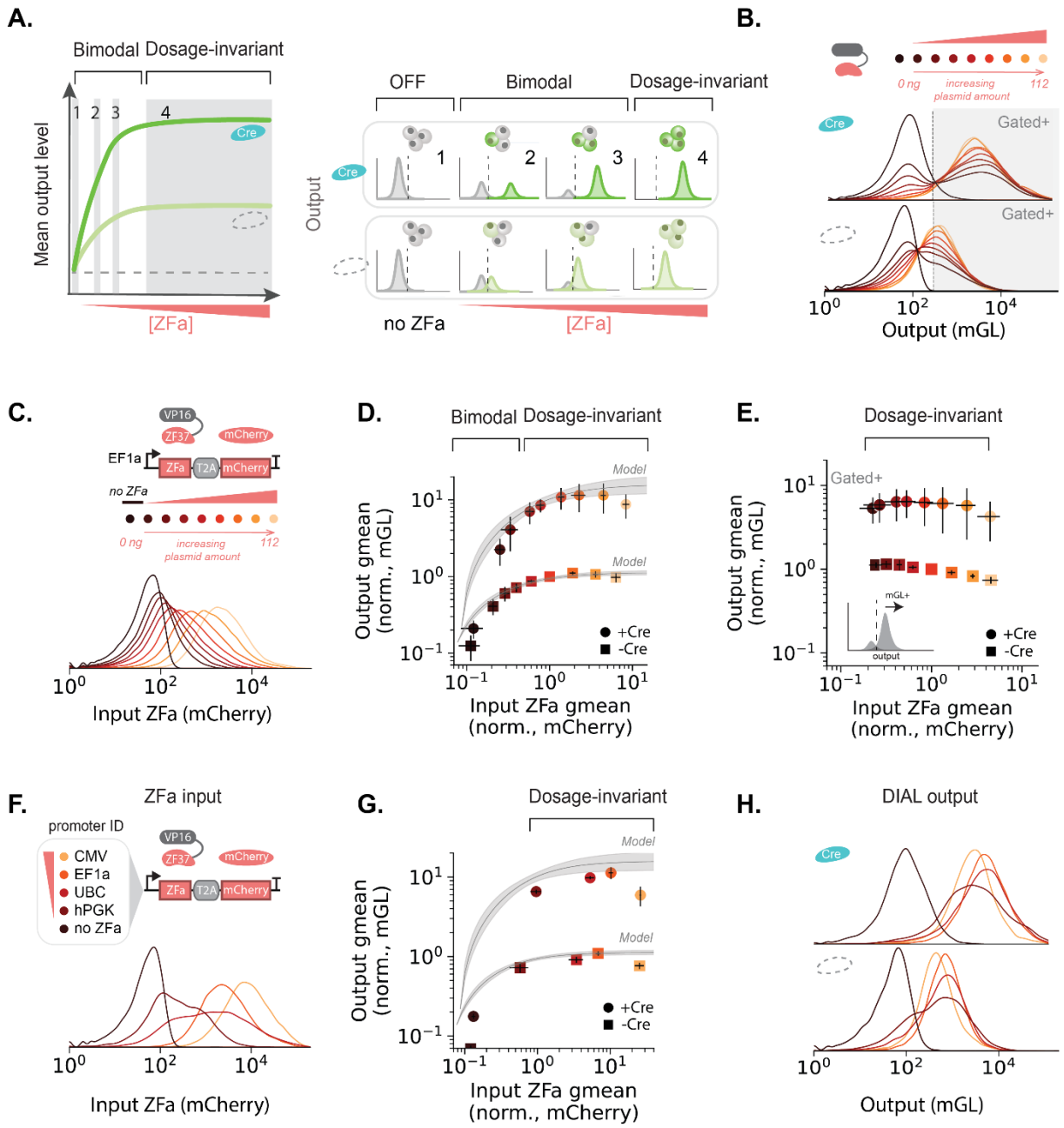

Figure 2. DIAL setpoints are robust to varying levels of ZFa.

(A) Schematic of ZFa (VP16-ZF37) titration. Low levels of ZFa result in a bimodal output regime, but beyond a certain threshold of ZFa level, the output levels enter a dosage invariant regime.
(B) Output mGL single-cell distributions from ZFa plasmid titration in transfection of HEK293T cells. Gate drawn (mGL-A>200) to identify cells with output fluorescence levels higher than cells with no ZFa.
(C) Schematic shows plasmid titration of ZFa. Histograms represent single-cell distributions of mCherry, co-expressed with titrated ZFa in transfection.
(D) Plot shows output mGL geometric MFI from the ZFa titration versus input ZFa geometric MFI (proxy by co-expressed mCherry) in transfection of HEK293T cells. Values are normalized to the condition without Cre with 0.125X (14 ng of ZFa). Overlaid lines represent model fits with 95% confidence interval. The output initial increases at low ZFa levels where the distribution is bimodal, followed by a dosage invariant regime.
(E) Data from ZFa plasmid titration in transfection of HEK293T cells as gated in the mGL channel by the line in (C). Plot shows output mGL geometric MFI versus input ZFa geometric MFI (tagged by mCherry) from the ZFa titration. Values are normalized to the condition without Cre with 0.125X (14 ng of ZFa). Once gated, the reporter output is dosage invariant throughout the ZFa plasmid titration.
(F) Schematic shows ZFa expressed by promoters of varying strengths in transfection of HEK293T cells. Histograms show single-cell distributions of ZFa input proxied by co-expressed mCherry.
(G) Plot shows output mGL geometric MFI versus input ZFa geometric MFI (proxied by mCherry) from different strength promoters for ZFa in transfection of HEK293T cells. Values are normalized to the condition without Cre of EF1a promoter added at 0.125X dilution (not shown). Overlaid lines represent model fits with 95% confidence interval. Output expression is invariant to ZFa dosage as titrated by different promoters.
(H) Histograms show output mGL single-cell distributions from ZFa with different promoters in transfection of HEK293T cells, colored according to legend in C.

All units for output MFI are a.u., and fold change is unitless. Large points in summary plots represent mean of transfection biological replicates -/+ standard error (n=6 plasmid titration, n=3 promoter strengths). Histograms represent single-cell distributions sampled across bioreplicates. Statistical significance was calculated with Students t-Test with ns $p>0.05$; *$p<0.05$; **$p<0.01$; *** $p<0.001$.

Figure 3. DIAL transmits transient inputs into heritable states.

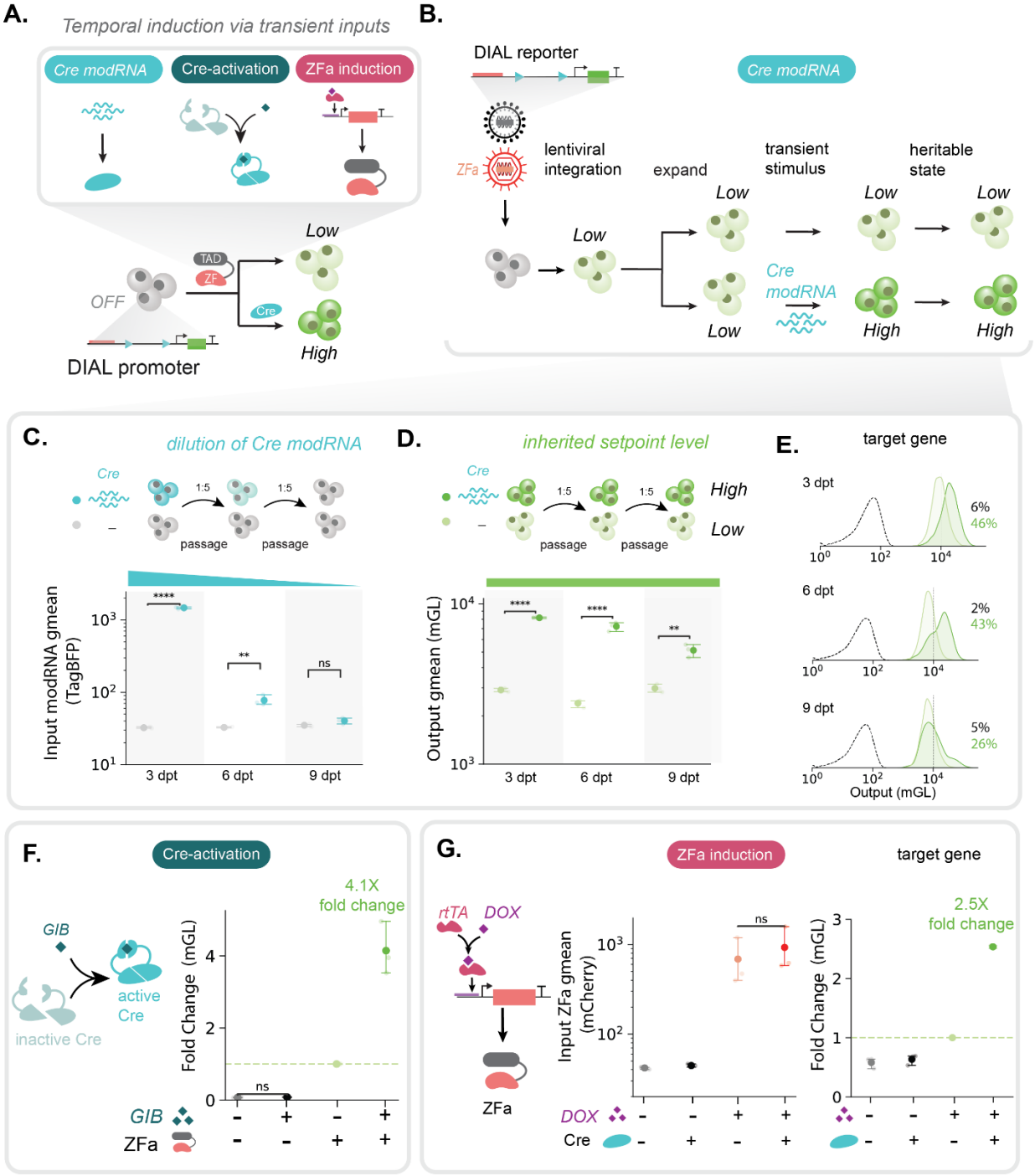

Figure 3. DIAL transmits transient inputs into heritable states.

(A) Schematic of different methods to control Cre and ZFa inputs in the DIAL promoter using transient external stimuli.

(B) Schematic of establishing a polyclonal HEK293T line with lentiviral-delivered ZFa and 203 bp spacer DIAL promoter regulating mGL, expansion, setting of expression level with and without modRNA Cre (transient stimuli), and inheritability of expression setpoint during proliferation.

(C, D, E) HEK293Ts with integrated ZFa and 203 bp spacer DIAL promoter regulating mGL were co-transfected with Cre modRNA and TagBFP modRNA on day 0.

(C) Plot shows TagBFP geometric MFI dilution over multiple passages as a proxy for Cre. TagBFP levels were measured on 3, 6, and 9 dpt. Transfected modRNA dilutes after multiple passages and dpt

(D, E) The output mGL setpoint level difference between conditions with and without Cre is inherited and persists across multiple passages. Plot shows geometric MFI of output target gene mGL over multiple passages gated for cells expressing mCherry (a proxy for ZFa). Histograms show single-cell distributions of output target gene mGL gated for mCherry. The dotted curve shows a negative population of HEK293Ts that does not expression the DIAL construct, ZFa, or mCherry.

(F) Schematic shows gibberellin-inducible split Cre, which was tested in transfection with ZFa and 203 bp DIAL promoter regulating mGL. Plots represent output mGL geometric MFI fold change from the condition without giberellin (GIB) and with ZFa. In the presence of GIB, activity of Cre increases which then increases expression of the output target gene, mGL, from the DIAL promoter.

(G) Schematic shows TRE3G promoter controlling expression of ZFa via doxycycline (DOX) induction. This construct was tested with plasmid-delivered Cre and 203 bp-spacer DIAL promoter regulating mGL. Plots show output geometric MFI of mCherry as a proxy for the ZFa (left) and output mGL geometric MFI fold change from the conditions with DOX and without Cre (right). DOX-inducible ZFa allows access to the off-state in addition to the low and high expression setpoints.

All units for output MFI are a.u., and fold change is unitless. Points in scatter plots represent mean of biological replicates -/+ standard error (n=3). Histograms represent single-cell distributions sampled across bioreplicates. Statistical significance was calculated with Students t-Test with ns $p>0.05$; *$p<0.05$; **$p<0.01$; *** $p<0.001$.

Figure 4. TET-DIAL system enables small-molecule activation of defined setpoints

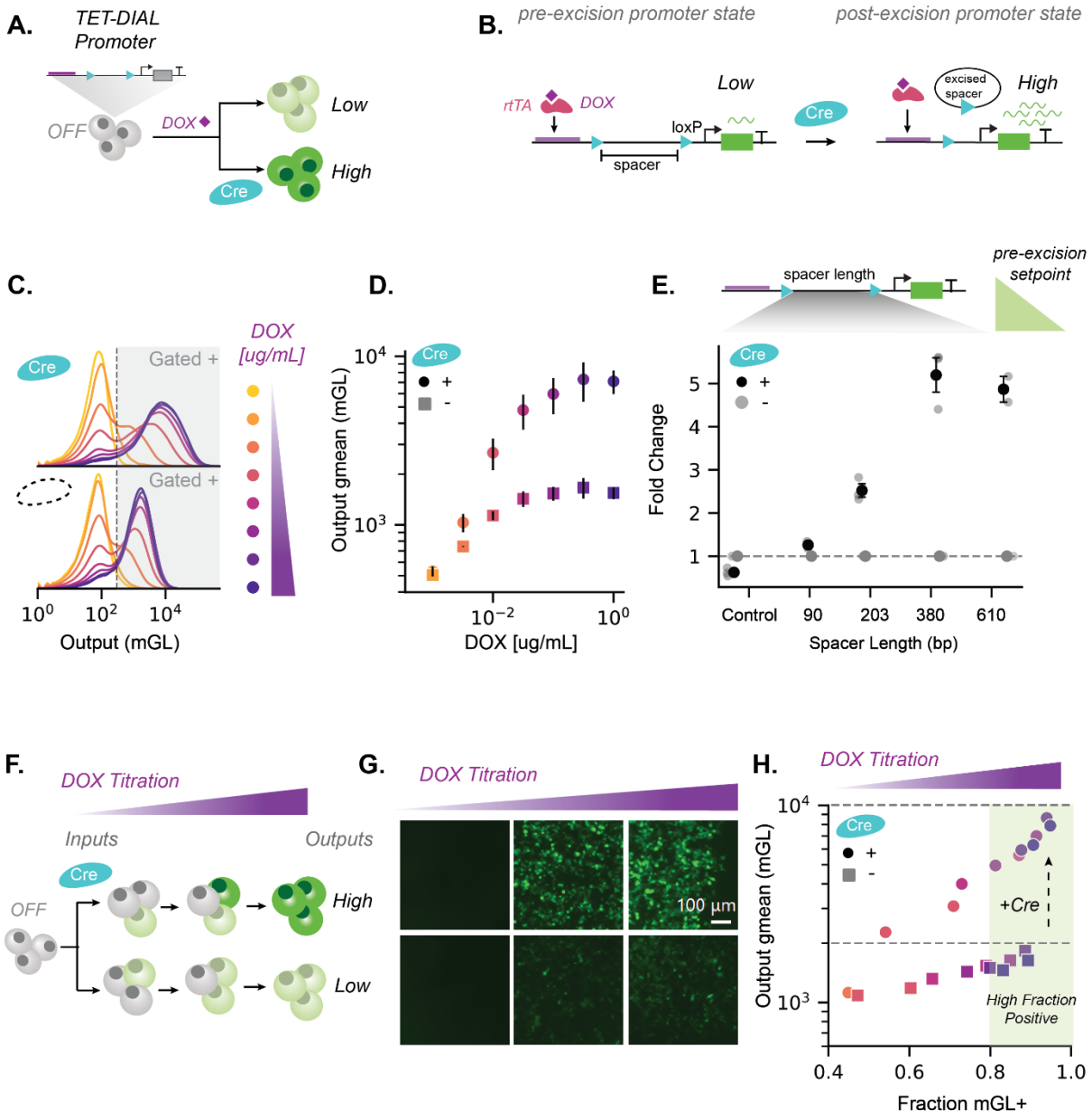

Figure 4. TET-DIAL system enables small-molecule activation of defined setpoints.

(A) Schematic of TET-DIAL promoter sequence co-delivered with rtTA under a constitute promoter generates three levels of gene expression in the presence of DOX and Cre.
(B) Schematic of TET-DIAL promoter with Cre-mediated excision of a floxed spacer of varying length. Excising the spacer increases expression of the target gene by reducing the distance from the activator domain to the minimal promoter.
(C) Representative output mGL single-cell distributions of DOX titration of 610 bp spacer TET-DIAL promoter regulating mGL, with and without Cre. The constructs were transiently transfected into HEK293Ts. Inclusion of Cre shifts the reporter mean to a higher level of expression whereas titrating DOX results concurrent changes in reporter positive cells and mean. Gate drawn at (mGL-A>200) to identify cells with output fluorescence levels higher than cells with no DOX.
(D) Scatter plot shows output mGL geometric vs. DOX concentration titration for transfected 610 bp-spacer TET-DIAL promoter regulating mGL with and without Cre. HEK293Ts were transiently transfected with TET-DIAL reporter, DOX induced 1 dpt, and flowed at 3 dpt.
(E) Fold changes for TET-DIAL promoter of varying spacer lengths regulating mGL at 1x DOX (1 ug/mL). All fold-changes normalized to the condition without Cre in each spacer length.
(F) Schematic of concurrent increase in fraction of reporter positive cells above the gate in C and means with DOX titration.
(G) Representative images of reporter expression in HEK293T cells ttransiently transfected with 203 bp-spacer TET-DIAL promoter regulating mGL in the absence (bottom) and presence of Cre (top) at varying DOX concentrations. Images taken at 3 dpt.
(H) Scatter plot of output mGL geometric MFI versus the fraction of cells above the gate in C for output reporter mGL from the 610 bp-spacer TET-DIAL promoter regulating mGL in the presence and absence of Cre transfected in HEK293T cells. Use of TET-DIAL allows for a shift between a low and high reporter expression state in the presence of Cre without compromising the fraction of mGL positive cells. Dashed lines separate low and high reporter expression regimes.

All units for output MFI are a.u., and fold change is unitless. Points in scatter plot D and summary plots represent mean of biological replicates -/+ standard error (n=3). Points in scatter plot H represent individual bioreplicates (n=3). Histograms represent single-cell distributions sampled across bioreplicates. Statistical significance was calculated with Students t-Test with ns $p>0.05$; *$p<0.05$; **$p<0.01$; *** $p<0.001$.

Figure 5. DIAL is extensible to different cell types and target genes

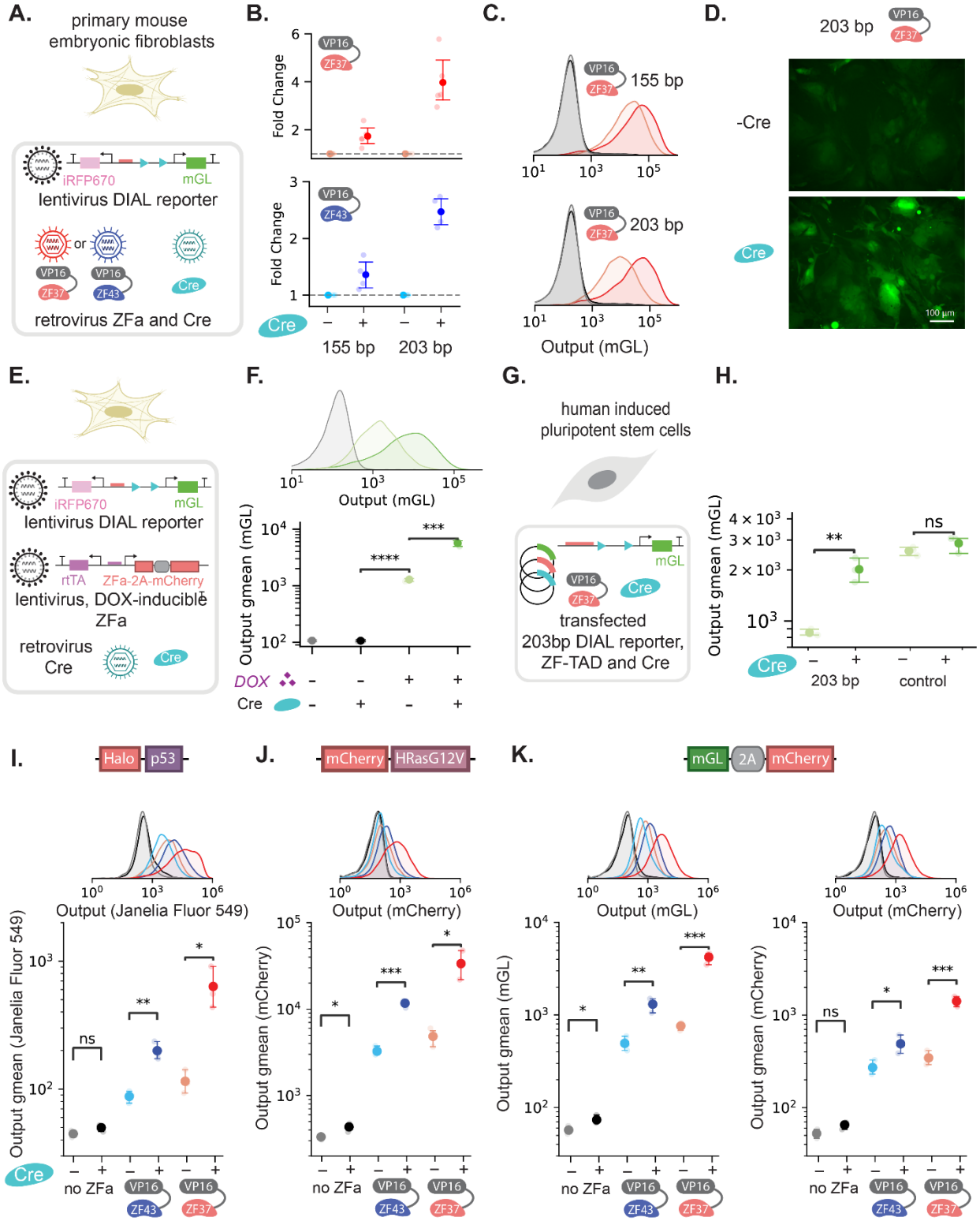

Figure 5. DIAL is extensible to different cell types and target genes

(A) Schematic of lentiviral-delivery of DIAL promoter regulating mGL with a divergent EF1a-iRFP670 to primary mouse embryonic fibroblasts (MEFs). Retroviruses constitutively expressing Cre, VP16-ZF37-2A-mCherry, and VP16-ZF43-2A-TagBFP can be delivered in combinations to set expression from the DIAL promoter.
(B) Fold change of mGL comparing the geometric MFI within each spacer length in the absence of Cre after gating on iRFP670+ and mGL+ within each spacer length. MEFs were infected as described in (A). Presence of Cre increases expression for both VP16-ZF37 and VP16-ZF43. Fold change increases with spacer length.
(C) Histograms represent single-cell distributions of data gated by iRFP670+ and additionally mCherry+ when there is presence of VP16-ZF37 retrovirus. MEFs were infected as described in (A). Legend follows (B), with an additional condition without ZF and with Cre (gray), and a condition both without ZF and Cre (black). Presence of ZFa turns on expression, and addition of Cre unimodally increases expression.
(D) Images 3 days post-infection (dpi) from MEFs viral infection using VP16-ZF37, 203 bp-spacer DIAL promoter regulating mGL, and with and without Cre as shown in (A). Increased expression in the presence of Cre is visualizable via microscopy.
(E) Schematic of lentiviral-delivered DIAL promoter regulating mGL with divergent EF1a-iRFP670 and DOX-inducible VP16-ZF37 to MEFs, with and without retroviral-delivered Cre.
(F) Histogram shows output mGL single-cell distribution from lentiviral-infection of MEFs as shown in E with DIAL promoter regulating mGL, DOX-inducible VP16-ZF37, and conditions with and without Cre. Plot shows output mGL geometric MFI with different combinations of DOX and Cre. DOX turns on output expression, and Cre increases expression from low to high.
(G) Schematic of plasmid transfection of VP16-ZF37, Cre, and DIAL promoter regulating mGL into iPSCs.
(H) iPSCs were transfected with 203 bp-spacer DIAL promoter or control DIAL promoter, as well as conditions with and without Cre. Data was gated on transfection marker. Plot shows output mGL geometric MFI where expression increases upon addition of Cre for the reporter containing a spacer.
(I) (I, J, K) 203 bp-spacer DIAL promoter regulating different target genes was transfected in HEK293Ts with different combinations of ZFa and Cre. The DIAL promoter changes expression for different target genes and all genes in a polycistronic cassettes.

Experiments were conducted with replicates (n=3 technical replicates in H, all others n=3 biological replicates) and analyzed as described in the Methods. Large plot points represent mean of individual transfections -/+ standard error. Histograms represent single-cell distributions sampled across replicates. Statistical significance was calculated with Students t-Test with ns $p>0.05$; *$p<0.05$; **$p<0.01$; *** $p<0.001$.

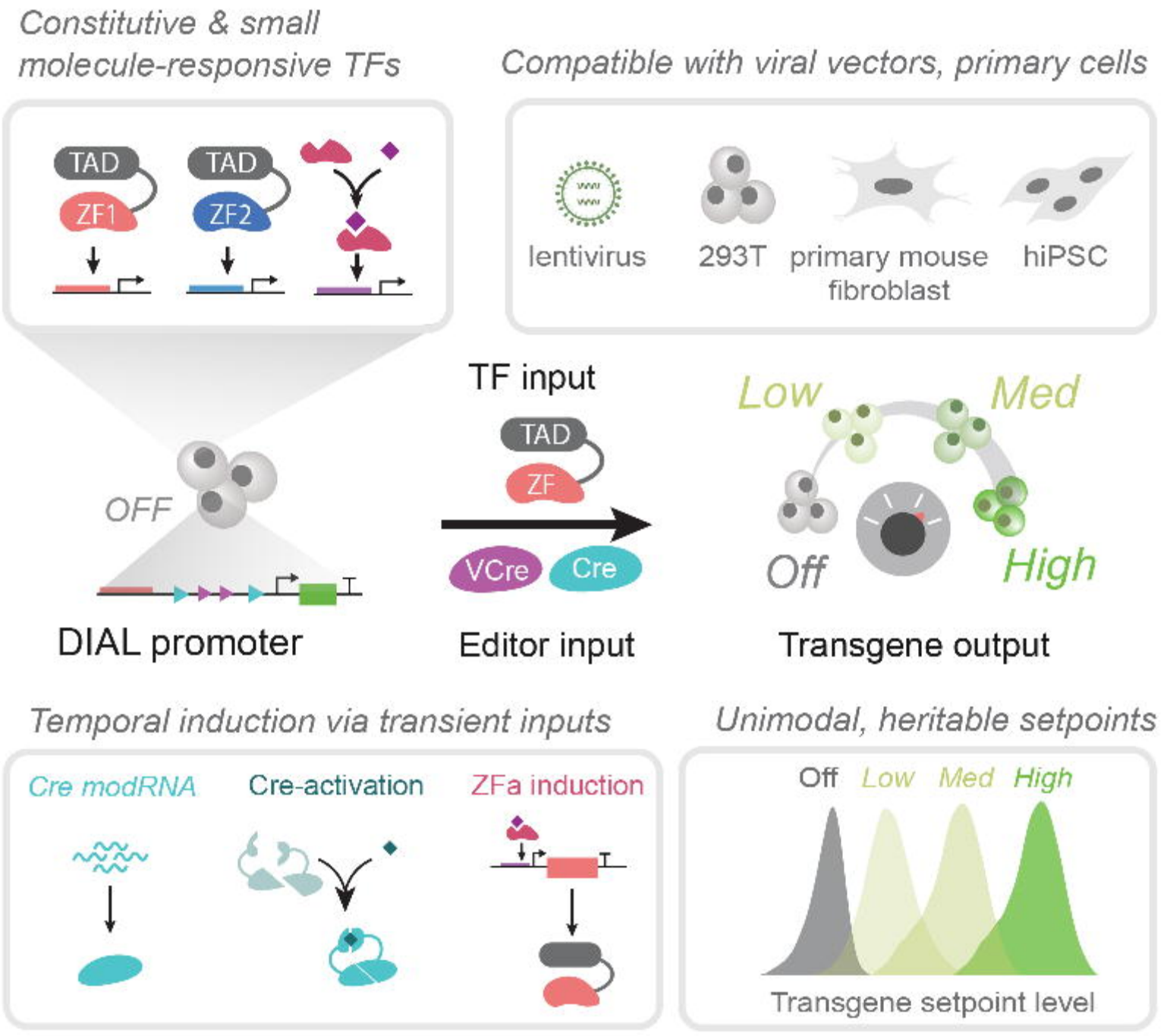
Constitutive & small molecule-responsive TFs
TAD
ZF1
TAD
ZF2
Compatible with viral vectors, primary cells
lentivirus
293T
primary mouse fibroblast
hiPSC
OFF
DIAL promoter
TF input
TAD
ZF
VCre
Cre
Editor input
Low
Med
Off
High
Transgene output
Temporal induction via transient inputs
Cre modRNA
Cre-activation
ZFa induction
Unimodal, heritable setpoints
Off
Low
Med
High
Transgene setpoint level

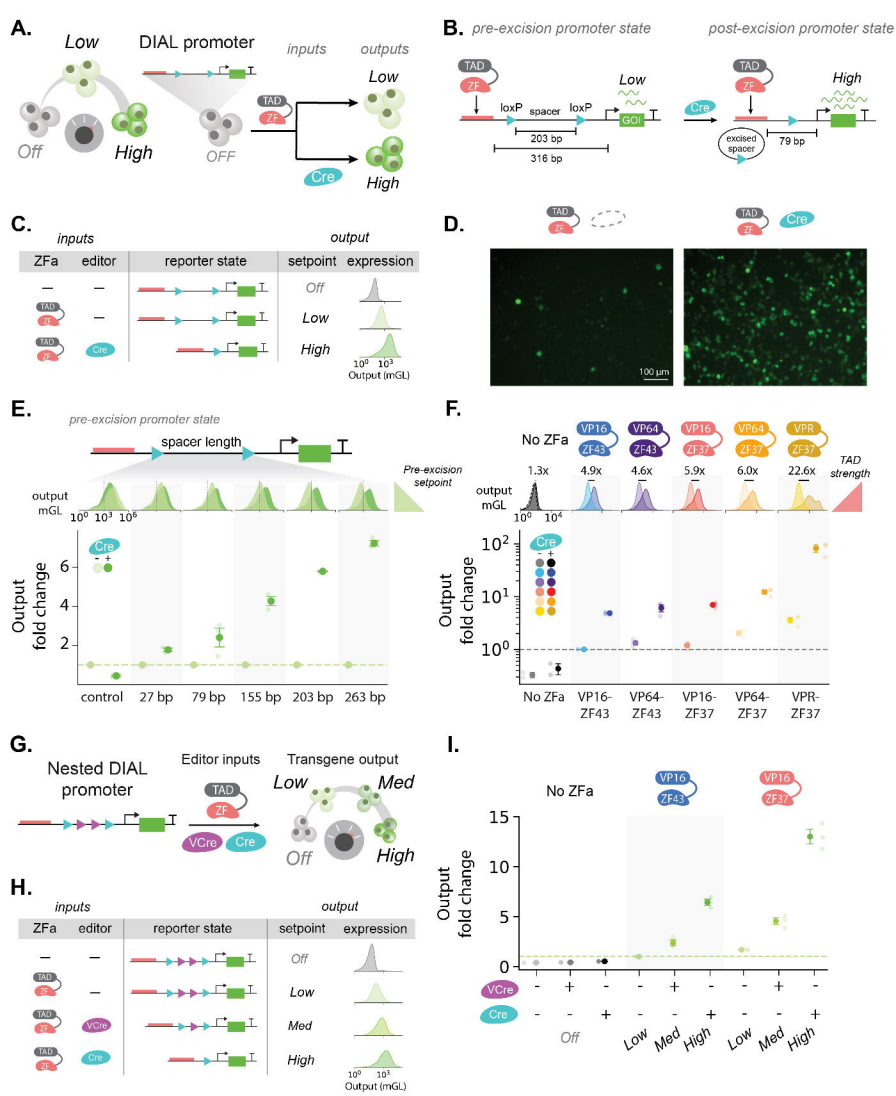
A.
Low
DIAL promoter
inputs
outputs
Off
High
OFF
TAD
ZF
Cre
Low
High
B.
pre-excision promoter state
post-excision promoter state
TAD
ZF
loxP
spacer
loxP
GOI
203 bp
316 bp
Low
Cre
excised spacer
79 bp
High
C.
inputs
output
ZFa
editor
reporter state
setpoint
expression
Off
Low
High
Cre
Output (mGL)
D.
TAD
ZF
Cre
100 µm
E.
pre-excision promoter state
spacer length
Pre-excision setpoint
output mGL
Output fold change
Cre
control
27 bp
79 bp
155 bp
203 bp
263 bp
F.
No ZFa
VP16 ZF43
VP64 ZF43
VP16 ZF37
VP64 ZF37
VPR ZF37
1.3x
4.9x
4.6x
5.9x
6.0x
22.6x
TAD strength
output mGL
Output fold change
Cre
No ZFa
VP16-ZF43
VP64-ZF43
VP16-ZF37
VP64-ZF37
VPR-ZF37
G.
Nested DIAL promoter
Editor inputs
Transgene output
TAD
ZF
VCre
Cre
Low
Med
Off
High
H.
inputs
output
ZFa
editor
reporter state
setpoint
expression
Off
Low
Med
High
VCre
Cre
Output (mGL)
I.
No ZFa
VP16 ZF43
VP16 ZF37
Output fold change
VCre
Cre
Off
Low
Med
High
Low
Med
High

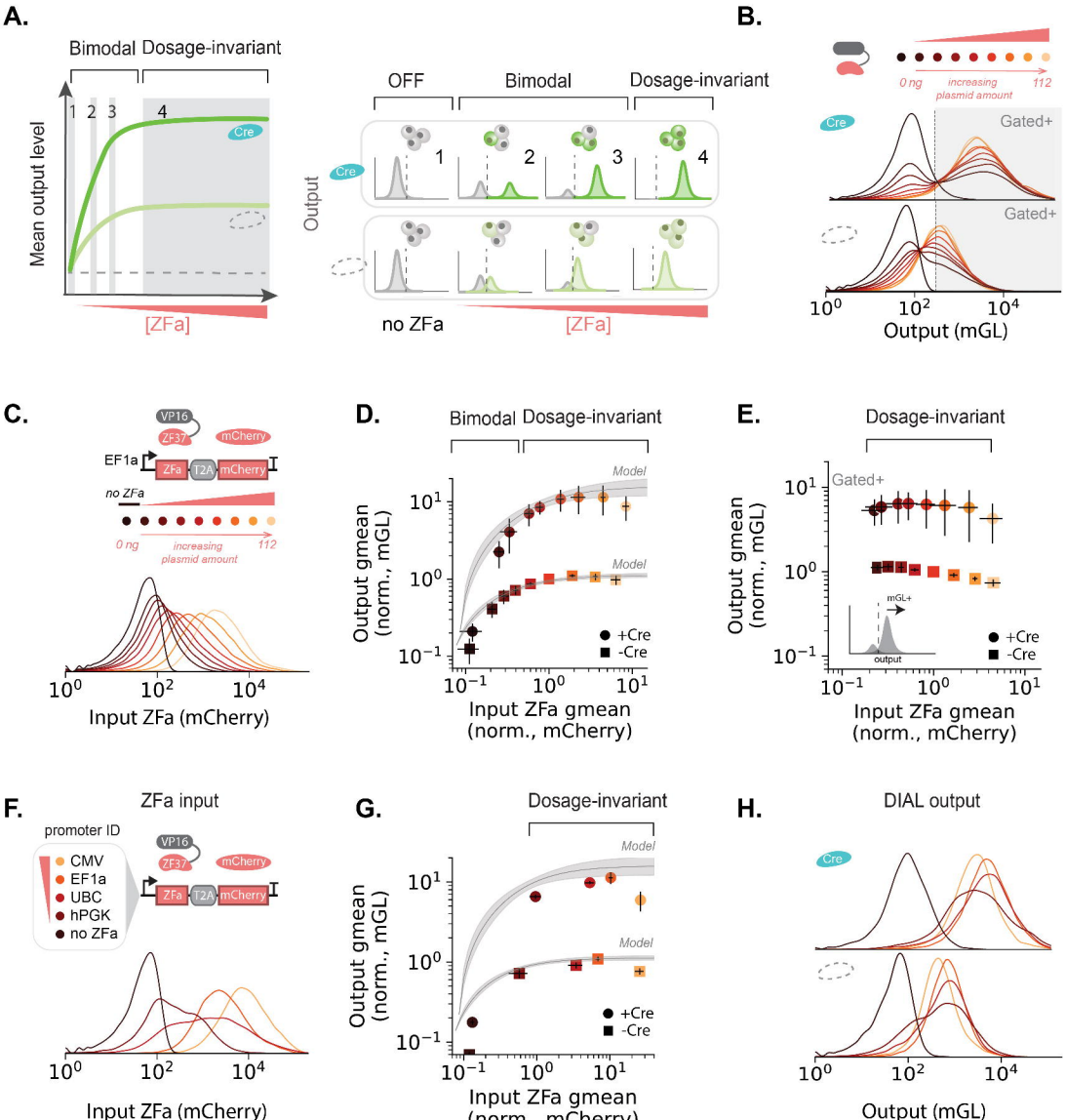
A.
Bimodal Dosage-invariant
Mean output level
1 2 3 4
Cre
[ZFa]
OFF
Bimodal
Dosage-invariant
Output
no ZFa
B.
0 ng
increasing plasmid amount
112
Gated+
Output (mGL)
C.
VP16
ZF37
mCherry
EF1a
ZFa
T2A
no ZFa
Input ZFa (mCherry)
D.
Model
Output gmean (norm., mGL)
+Cre
-Cre
Input ZFa gmean (norm., mCherry)
E.
Dosage-invariant
mGL+
output
F.
ZFa input
promoter ID
CMV
EF1a
UBC
hPGK
no ZFa
G.
H.
DIAL output

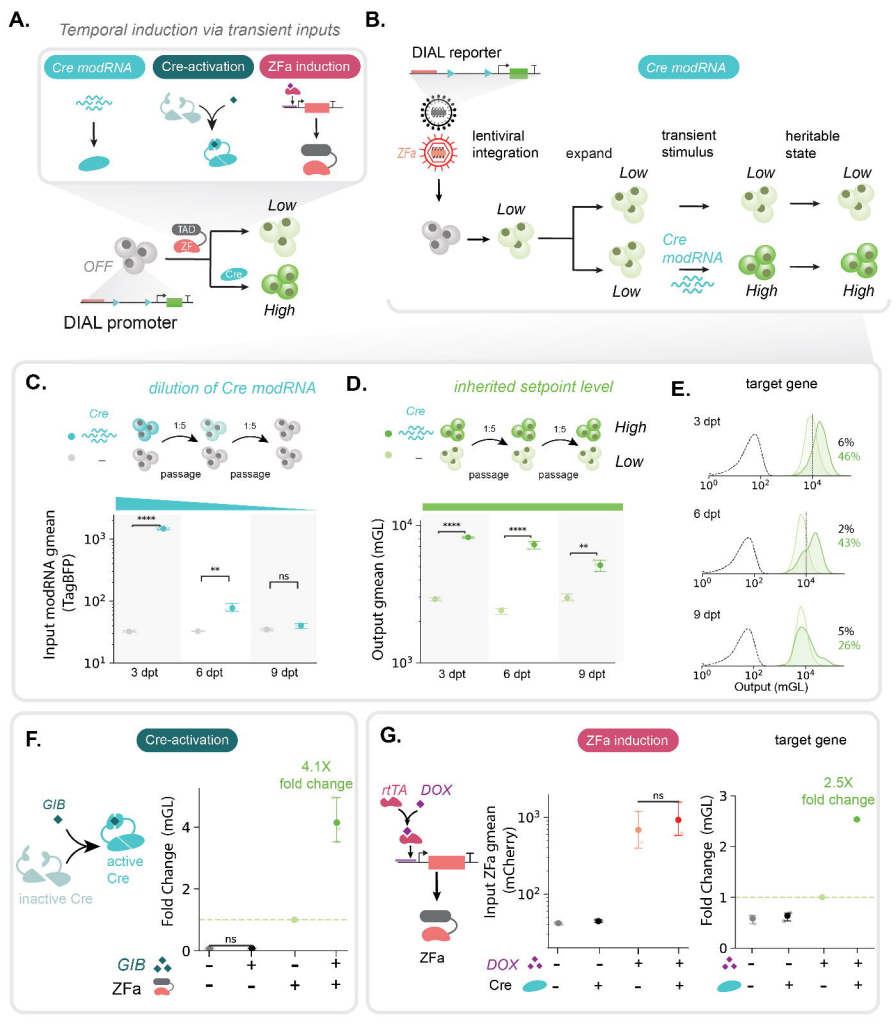
A.
Temporal induction via transient inputs
Cre modRNA
Cre-activation
ZFa induction
OFF
TAD
ZF
Cre
Low
High
DIAL promoter
B.
DIAL reporter
Cre modRNA
ZFa
lentiviral integration
expand
transient stimulus
heritable state
Low
Cre modRNA
High
C.
dilution of Cre modRNA
Cre
1:5
passage
Input modRNA gmean (TagBFP)
3 dpt
6 dpt
9 dpt
D.
inherited setpoint level
High
Low
Output gmean (mGL)
E.
target gene
6%
46%
2%
43%
5%
26%
Output (mGL)
F.
Cre-activation
GIB
active Cre
inactive Cre
4.1X fold change
Fold Change (mGL)
ns
ZFa
G.
ZFa induction
target gene
rtTA
DOX
Input ZFa gmean (mCherry)
2.5X fold change
Cre

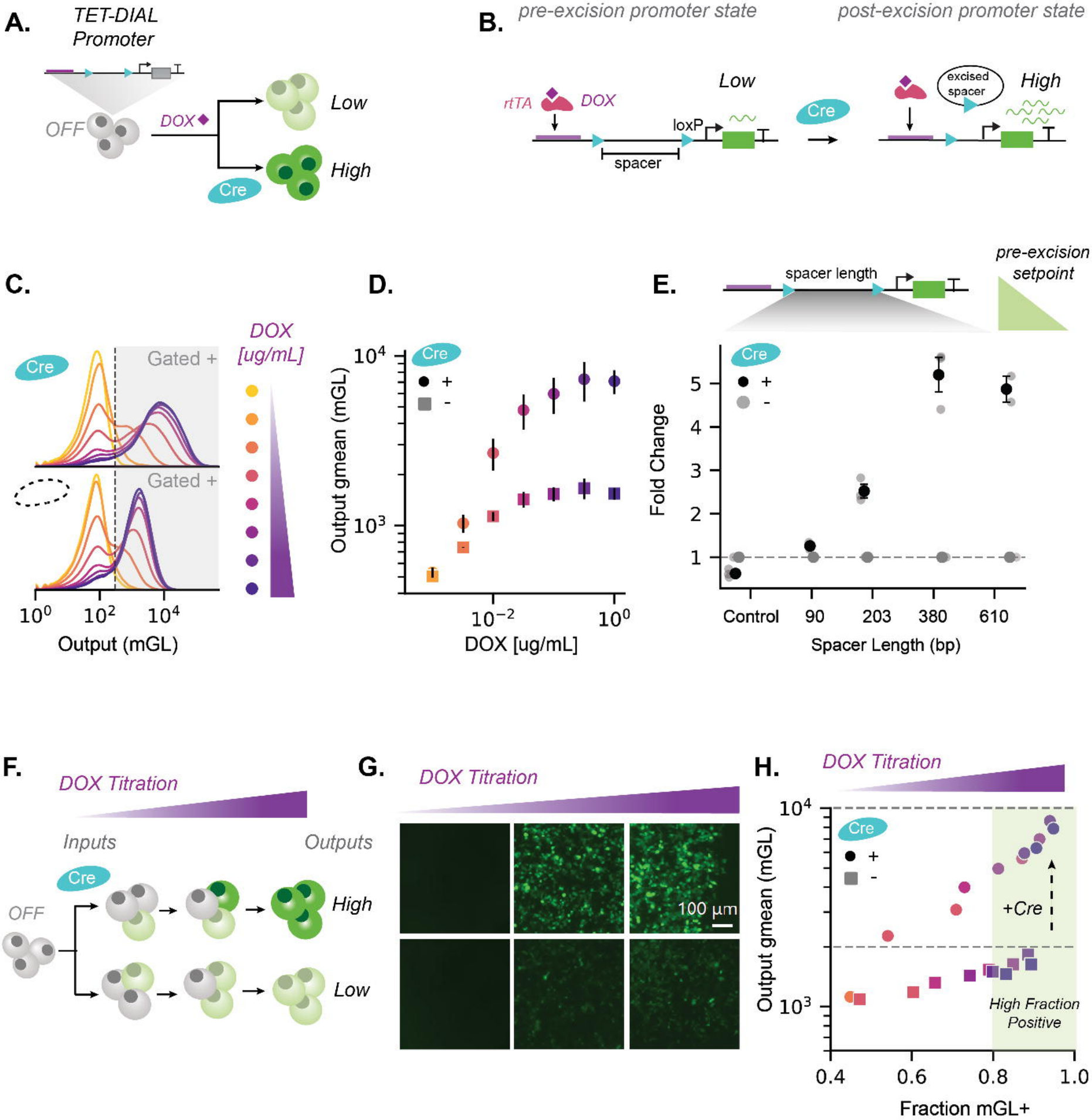
A.
TET-DIAL Promoter
OFF
DOX
Low
High
Cre
B.
pre-excision promoter state
post-excision promoter state
rtTA
DOX
Low
loxP
spacer
Cre
excised spacer
High
C.
Cre
Gated +
Gated +
DOX [ug/mL]
Output (mGL)
D.
Cre
+
-
Output gmean (mGL)
DOX [ug/mL]
E.
spacer length
pre-excision setpoint
Cre
+
-
Fold Change
Control
90
203
380
610
Spacer Length (bp)
F.
DOX Titration
Inputs
Outputs
Cre
OFF
High
Low
G.
DOX Titration
100 µm
H.
DOX Titration
Cre
+
-
+Cre
High Fraction Positive
Output gmean (mGL)
Fraction mGL+

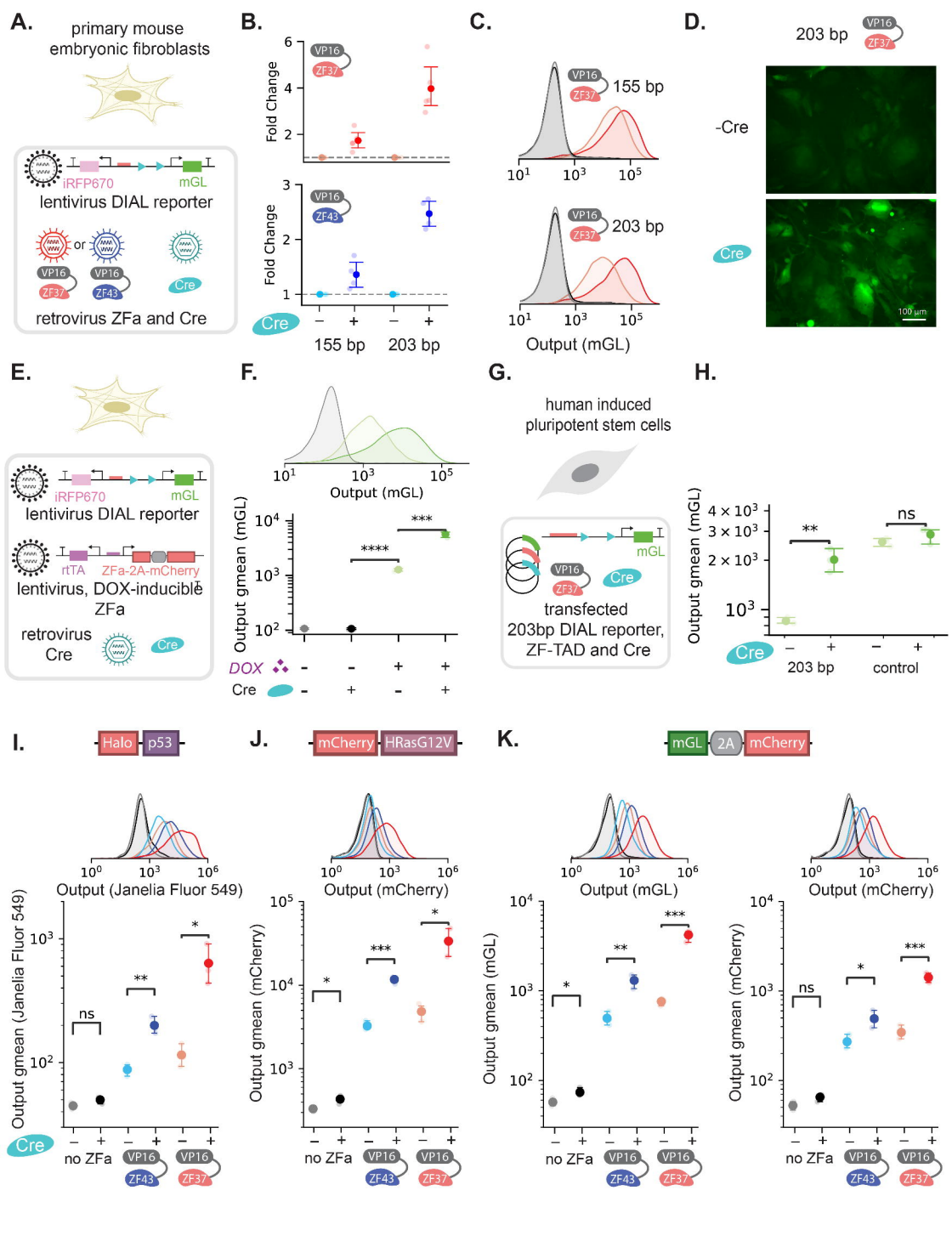
A.
primary mouse embryonic fibroblasts
iRFP670
mGL
lentivirus DIAL reporter
or
VP16
ZF37
VP16
ZF43
Cre
retrovirus ZFa and Cre
B.
Fold Change
VP16
ZF37
VP16
ZF43
Cre
155 bp
203 bp
C.
VP16
ZF37
155 bp
203 bp
Output (mGL)
D.
203 bp
-Cre
Cre
100 µm
E.
iRFP670
mGL
lentivirus DIAL reporter
rtTA
ZFa-2A-mCherry
lentivirus, DOX-inducible ZFa
retrovirus Cre
Cre
F.
Output (mGL)
Output gmean (mGL)
DOX
Cre
G.
human induced pluripotent stem cells
mGL
VP16
ZF37
Cre
transfected 203bp DIAL reporter, ZF-TAD and Cre
H.
Output gmean (mGL)
203 bp
control
Cre
I.
Halo
p53
Output (Janelia Fluor 549)
Output gmean (Janelia Fluor 549)
no ZFa
VP16 ZF43
VP16 ZF37
Cre
J.
mCherry
HRasG12V
Output (mCherry)
Output gmean (mCherry)
K.
mGL
2A
mCherry
Output (mGL)
Output gmean (mGL)
Output (mCherry)
Output gmean (mCherry)